WATER RESOURCES RESEARCH, VOL. 46, W03514, doi:10.1029/2009WR008371, 2010

Transport in the hydrologic response: Travel time distributions, soil moisture dynamics, and the old water paradox

Gianluca Botter,[1] Enrico Bertuzzo,[2] and Andrea Rinaldo[1,2]

Received 8 July 2009; revised 23 October 2009; accepted 29 October 2009; published 12 March 2010.

[1] We propose a mathematical framework for the general definition and computation of travel time distributions defined by the closure of a catchment control volume, where the input flux is an arbitrary rainfall pattern and the output fluxes are green and blue water flows (namely, evapotranspiration and the hydrologic response embedding runoff production through soil water dynamics). The relevance of the problem is both practical, owing to implications in hydrologic watershed modeling, and conceptual for the linkages and the explanations the theory provides, chiefly concerning the role of geomorphology, climate, soils, and vegetation through soil water dynamics and the treatment of the so-called old water paradox. The work focuses in particular on the origins of the conditional and time-variant nature of travel time distributions and on the differences between unit hydrographs and travel time distributions. Both carrier flow and solute matter transport in the control volume are accounted for coherently. The key effect of mixing processes occurring within runoff production is also investigated, in particular by a model that assumes that mobilization of soil water involves randomly sampled particles from the available storage. Travel time distributions are analytically expressed in terms of the major water fluxes driving soil moisture dynamics, irrespectively of the specific model used to compute them. Relevant numerical examples and a set of generalized applications are provided and discussed.

Citation: Botter, G., E. Bertuzzo, and A. Rinaldo (2010), Transport in the hydrologic response: Travel time distributions, soil moisture dynamics, and the old water paradox, *Water Resour. Res.*, *46*, W03514, doi:10.1029/2009WR008371.

1. Introduction

[2] The age of water (or residence time) represents the time spent by water molecules ideally sampled from a given hydrologic system within the reference control volume (measured since the entry through rainfall). Thus, the age of water blends in a single quantitative attribute information about hydrological and chemical storages, flow pathways, and water sources [e.g., *McGuire and McDonnell*, 2006]. Several field observations (especially built through extensive rainfall/runoff dating by isotope hydrology) and a few theoretical results have established the so-called "old water paradox," according to which a sizable part of the runoff within the hydrologic response of catchment transport volumes is constituted by aged water particles (i.e., by water particles injected at times preceding the event causally related to the observed runoff) [e.g., *Maloszewski and Zuber*, 1982; *McDonnell*, 1990; *McDonnell et al.*, 1991; *Stewart and McDonnell*, 1991; *Wilson et al.*, 1991a, 1991b; *Leaney et al.*, 1993; *Rodhe et al.*, 1996; *Cirmo and McDonnell*, 1998; *Nyberg et al.*, 1999; *Peters and Ratcliffe*, 1998; *Burns et al.*, 1998; *Weiler et al.*, 2003; *McGuire et al.*, 2007; *Botter et al.*, 2007, 2008a, 2009]. The release of old water has been explained by the propagation of pressure waves induced by precipitation inputs with a celerity exceeding the pore water velocity [e.g., *Beven*, 1981, 1989b], including displacement of water previously immobilized within the soil matrix into preferential flow pathways [e.g., *Beven and Germann*, 1982]. However, some of the physical processes controlling the release of preevent water from catchments are still poorly understood or roughly modeled, and the observational data do not suggest either universal behaviors, nor do they support linear and time-invariant behaviors as assumed by unit hydrograph schemes [e.g., *Weiler and McDonnell*, 2006]. The complexity of the mixing patterns involving event and preevent waters in hillslopes is partly a byproduct of the structural complexity of subsurface environments, which are typically characterized by pronounced heterogeneity and time variable connectivity of flow pathways. For this reason, it is inappropriate to use the point-scale physical laws determining the movement of water and solutes within hillslopes to make predictions at larger scales because of the nonlinearity of flow processes and the uncertain distribution of hydrologic, geological and morphological properties of control volumes [e.g., *Beven*, 1989a, 2006; *Kirchner*, 2009]. Hence, lumped approaches are frequently employed to describe in an effective manner the overall behavior of hillslopes/catchments. In particular, the water travel time

[1]Dipartimento di Ingegneria Idraulica Marittima Ambientale e Geotecnica, Università degli Studi di Padova, Padua, Italy.
[2]Laboratory of Ecohydrology, Faculté ENAC, Ecole Polytechinque Federale, Lausanne, Switzerland.

0043-1397/10/2009WR008371

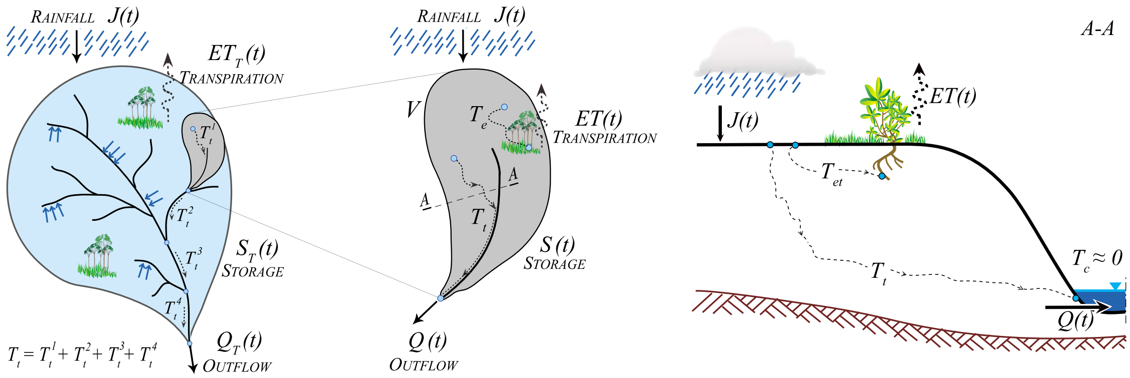

Figure 1. Schematic representation of the control volume V within which transport processes are analyzed. (left) An entire catchment where individual travel times are additive and composed geomorphically by serial and parallel arrangement through path probabilities. (middle) The actual transport volume V considered in this study, chiefly composed of unchanneled areas. Note that the patchwork of such transport volumes covers the catchment. (right) A cross section of V emphasizing the key components of exit time, the evapotranspiration time (T_e) and the travel time (T_t).

(i.e., the time spent by water while traveling through a hillslope/catchment from the entrance to the passage across the outlet) is a major lumped descriptor of the flow and transport dynamics taking place in heterogeneous hydrologic systems [e.g., *Dagan*, 1989; *Cvetkovic and Dagan*, 1994; *Rinaldo et al.*, 2006a; *McGuire and McDonnell*, 2006, and references therein]. The probability distribution function (pdf) of travel times, in fact, provides a stochastic (and mathematically robust) description of how catchments retain and release water, and has the major advantage of blending all sources of uncertainty (e.g., the description of the spatial patterns of soil hydraulic properties) into a single curve [*Taylor*, 1921; *Dagan*, 1989], albeit that this will, in the general case, be time variable. Thus, travel times qualify as the key variable for quantifying the fraction of preevent water composing the streamflows. Exploring the roles of geomorphology, soils, climate and vegetation in shaping the whole distribution of travel times sheds light on how catchment properties control its chemical and hydrologic responses [e.g., *Rodriguez-Iturbe and Valdes*, 1979; *Gupta et al.*, 1980; *Rinaldo and Marani*, 1987; *Rinaldo et al.*, 1989, 1991; *Rodhe et al.*, 1996; *Weiler et al.*, 2003; *McGuire et al.*, 2007; *Fiori and Russo*, 2008].

[3] These issues are obviously relevant to models of the hydrologic response, but become particularly important for solute transport schemes at basin scales, as the chemical composition of the water particles released from a hillslope (or catchment) is significantly affected by their actual travel times in the case of both reactive and nonreactive solutes. For nonreactive solutes the travel time distribution allows a proper quantification of the persistence of the chemical signatures of past rain events in the streamflow concentration. In the case of reactive solutes, instead, travel times are important drivers of the solute transformations occurring along hydrologic pathways, which are possibly induced by chemical, physical or biological processes between (and within) mobile or immobile water/soil phases.

[4] From this perspective, the watershed acts as an integrator of flows whose ages and solute matter contents are heterogeneous depending on sources, origins, nature of the soil and channel states visited in the hydrologic journey to the basin outlet. Thus, the release of old water during rainfall events is a key factor to explain the difference observed between the time scale characterizing the unit hydrograph and that of the travel time distribution [e.g., *Weiler et al.*, 2003; *McGuire and McDonnell*, 2006; *Fiori and Russo*, 2008]. Indeed, the difference between the above two responses apparently calls into question traditional causal approaches based on instantaneous unit hydrograph schemes and the Taylorian formulation of transport by continuous movements [*Rodriguez-Iturbe and Valdes*, 1979; *Gupta et al.*, 1980; *Rinaldo and Marani*, 1987; *Rodriguez-Iturbe and Rinaldo*, 1997; *Rinaldo et al.*, 2006a, 2006b; *Botter et al.*, 2005, 2009], suggesting the need for a reassessment.

[5] This paper attempts a theory of transport in the hydrologic response by reformulating Taylor's theorem to account for nonlinearities induced by time-varying rainfall, runoff and evapotranspiration processes. To this aim, we employ conditional travel time pdf's for reactive and nonreactive matters, that generalize previous schemes of mass response functions [*Rinaldo and Marani*, 1987; *Rinaldo et al.*, 1989, 2006a, 2006b; *Botter et al.*, 2005, 2006, 2008a, 2009]. The difference between the unit hydrograph and the travel time distribution is then addressed in a coherent mathematical framework by introducing suitable waiting time pdf's expressing the age of the effective rainfall. We also investigate the mixing processes occurring in hillslopes within the runoff generation (with particular attention to the mixing occurring in the root zone), and the dependence of the travel time distribution on the underlying soil, vegetation and climate features of the catchment.

[6] At no loss of generality, in this work we focus only on the response of single control volumes, which represent individual hillslopes (or small catchments characterized by rudimentary geomorphic structures). In fact, under the further (mild) assumption of statistical independence of travel times within different geomorphic states (say, within a hillslope and its downstream draining channels) and because of the additive nature of travel times in serial control volumes (see Figure 1), the probability distribution describing first passages at the closure of complex watersheds can be obtained by

convolution of the individual probability distributions of travel times within each component. Arbitrary serial and parallel arrangements of geomorphic states could thus be tackled in a straightforward manner through suitable path probabilities [*Rodriguez-Iturbe and Valdes*, 1979: *Gupta et al.*, 1980], possibly time dependent owing to rainfall patterning [*Rinaldo et al.*, 2006a].

[7] The paper is organized as follows. Section 2 establishes the theoretical background and the basic relation of volume-integrated mass balance equations with the travel time formulation of transport. Therein, a first example were evapotranspiration is neglected highlights the difference between unit hydrographs and exit time pdf's. Section 3 extends the framework to the case when output fluxes include both runoff and evapotranspiration. Section 4 deals with how the description of reactive and nonreactive compounds transported by the water carrier can be included. We then address (section 5) the relation of the new tools with unit hydrographs by introducing a suitable waiting time pdf. Subsequently (section 6), we develop a simplified stochastic model for the mixing occurring in the root zone within and between runoff events, which allows the derivation of an analytical expression for the travel time pdf. The analysis of the results obtained from a series of numerical simulations is presented in section 7. A brief discussion of some relevant generalizations of the scheme (section 8) and a set of conclusions then closes the paper.

2. Theoretical Framework: Exit Time Pdf's and Unit Hydrographs

[8] The approach starts from the definition of a well-defined control volume V (Figure 1), which represents a hillslope, a catchment or a subcatchment of a river basin. Given that at the spatial scales typical of large catchments, in-stream processes, such as hyporheic exchanges and interactions with riparian zones, can strongly impact flow and transport features observed at the outlet [e.g., *Lindgren et al.*, 2004; *Mulholland et al.*, 2008], we shall focus here only on relatively small catchments where the effect of the channel network on the processes of interest can be neglected. The response of large catchments, however, could be derived in the same framework by including the geomorphic effect due to the actual arrangement of subcatchments around the channel network, and the relevant in-stream processes. The control volume V is bounded by the catchment/hillslope surface through which water particles enter V as precipitation, a no flux lateral surface defined by the catchment divides, and the outlet collecting the hydrologic response, typically a compliance surface (a channel cross section) at the catchment closure acting as absorbing barrier for the water particles composing the hydrologic response. Deep losses and recharge terms supplying deep groundwater bypassing the catchment control section will be neglected here for simplicity and to avoid clouding the main issue with unnecessary details.

[9] Under the above assumptions, the most relevant processes affecting the time evolution of water and solute storage in the control volume V (denoted as $S(t)$ and $M(t)$, respectively) are precipitation, evapotranspiration and soil drainage, as discussed below.

[10] 1. Precipitation represents the only input for the system under consideration and contributes to increase the water storage during rainfall events, controlled by the temporal variability of the rainfall rates $J(t)$. It may also affect the solute storage, however, as commanded by the temporal variability of the rainfall solute concentration $C_0(t)$;

[11] 2. Evapotranspiration $ET(t)$ represents the sum of the output fluxes due to soil evaporation (triggered by solar radiation and affected by climatic features and soil water availability) and plant transpiration (which depends primarily on climatic and vegetation features, besides water availability). Because in vegetated soils the fraction of water mass which evaporates from the soil is usually smaller than the fraction of water mass transpired by plants, in what follows we will focus on overall estimates of transpiration processes. The solute uptake associated with transpiration, $\phi_{ET}(t)$ depends on the specific solute specie considered, and on the plants ability to incorporate chemicals from the soil solution in a selective manner;

[12] 3. Drainage toward the channel network is usually triggered by subsurface gradients of soil water potential. Connectivity of soil regions characterized by high permeability, heterogeneity of the underlying morphologic and hydraulic properties, presence/absence, depth and perviousness of a bedrock, nonlinear dependence of the local velocities on the soil water content are all features having a strong impact on the water flux leaving the control volume as streamflow, $Q(t)$ (and on the solute flux associated with Q, $\phi_Q(t)$).

[13] The mass balance equations driving the temporal evolution of the water and solute storages in the control volume V can be thus expressed as

$$\frac{dS(t)}{dt} = J(t) - Q(t) - ET(t), \tag{1}$$

$$\frac{dM(t)}{dt} = \phi_0(t) - \phi_Q(t) - \phi_{ET} + \left(\frac{dM}{dt}\right)_{react}, \tag{2}$$

where $\phi_0(t) = J(t)C_0(t)$ is the solute input through rainfall, and $\phi_Q(t) = Q(t)C_F(t)$ is the solute flux exiting V through streamflows (C_F being the flux concentration of solute matter in streamflows). The term $(dM/dt)_{react}$ in equation (2) defines arbitrary exchange terms affecting the mass balance of reactive solutes involved in biological, chemical or physical transformations (e.g., biogeochemical cycling or any mass transfer from mobile or immobile water or soil phases). Equations (1) and (2) constitute a set of coupled equations, the coupling being inherent in the dependence of the solute fluxes ϕ_Q, ϕ_{ET}, ϕ_0 on the corresponding water fluxes Q, ET and J.

[14] Transport features within V are described through exit times of the individual water particles into which the input can be ideally subdivided. Notwithstanding different definitions that have been provided in the literature [e.g., *McGuire and McDonnell*, 2006], in this paper the exit time of a given water particle (T_{ex}) is defined as the time elapsed between the entrance of such particle within V and its exit through any boundary of the control volume. T_{ex} is thought of as a random variable characterized by a given pdf, say $p_{ex}(t)$. A key point is that, in general, the fate of the injected water particles (i.e., their exit time T_{ex}) depends on the time at which the injection into V of such particles occurs (evaluated with respect to a given time origin), say T_i. This

dependence can be heuristically explained as follows: the water particles entering V during periods when the storage is small are most likely to be retained inside V for longer times than particles which enter V when the system is close to saturation, because of the nonlinear dependence of the output fluxes on the storage. If the input forcing is conceptualized as a sequence of water particles injected in V at different times, T_i can be seen as a random variable whose probability density function is proportional to J. Therefore, the dynamics taking place in V could be properly described by specifying the joint probability distribution function of T_i and T_{ex}. Alternatively, one can prescribe the input rate $J(t)$ (i.e., the pdf of T_i) and the probability density function of T_{ex} conditional to the injection time t_i, $p_{ex}(t|t_i)$. The latter, in general, must depend on the system state at injection and on the sequence of states experienced afterwards (hence on the structure of the whole input J). To emphasize this fact, the notation $p_{ex}(t|t_i; J)$ will be employed (i.e., $p_{ex}(t|t_i; J)dt$ represents the fraction of water particles injected in t_i, the exit time of which falls in the interval $[t, t + dt]$). Accordingly, let $P_{ex}(t|t_i; J)$ be the exceedance cumulative probability of exit time for the water particles which have entered V at t_i (i.e., $P_{ex}(t|t_i; J) = 1 - \int_0^t p_{ex}(x|t_i; J)dx$).

[15] To better highlight the differences between the hillslope/catchment hydrograph response and the underlying exit time distribution, we will shall first consider the simplified case in which evapotranspiration is neglected ($ET = 0$) and the whole rainfall input J is effective in terms of streamflow production (i.e., the outflow volume is assumed to be equal to the rainfall volume for any single event, and, therefore, the water storage before and after the event is the same). Under the above assumptions, equation (1) becomes

$$\frac{dS}{dt} = J(t) - Q(t), \tag{3}$$

where J corresponds to an effective rainfall series. Let $h(t)$ be the unit hydrograph, which defines the temporal distribution of the output produced by a given (effective and unit) rainfall pulse, evaluated from the occurrence of the pulse. Under the linearity assumption, on which the unit hydrograph theory is based, the outflow $Q(t)$ can be expressed as the convolution between J and h (e.g., *Sherman* [1932]; for a general introduction of the subject see *Beven* [2001])

$$Q(t) = \int_{-\infty}^{t} J(t_i)h(t - t_i)dt_i. \tag{4}$$

[16] Note that to avoid clouding our main point, we have assumed in equation (4) the unit hydrograph h as time invariant (and thus dependent on a single time scale). This assumption, however, is not functional to our results and can be relaxed. The linear approach underlying equation (4) provides a causal relationship between the effective rainfall and Q (see Figure 2), taking into account the stochastic nature of the transport processes, and it may include the dispersive effects induced by the heterogeneity of soil properties or arbitrary geomorphic complexity [*Rodriguez-Iturbe and Valdes*, 1979; *Gupta et al.*, 1980; *Rinaldo et al.*, 1991]. The scheme is known to provide a framework to develop simple and effective rainfall-runoff models. However, in general the unit hydrograph h differs consistently from the exit time distribution, p_{ex}, except for some special cases (e.g., the case of zero storage at the start of each event). In fact, in the unit hydrograph formulation, there is no requirement that the input and the output waters be the same (that is, the output produced by a given rainfall pulse may be in general constituted also by water particles already stored in the control volume before the storm, and displaced during the considered event). Thus, the age of runoff cannot be properly captured through this formulation.

[17] To consider the effective age of the water particles leaving V via Q, it is necessary to reformulate the mass balance equation in Lagrangian terms by using the exit time distribution, p_{ex}. According to the definitions given above, the quantity $P_{ex}(t - t_i|t_i; J)$ represents the probability that a water particle injected at time t_i is still within the control volume at time t. Thus, the instantaneous water storage $S(t)$ can be expressed as

$$S(t) = \int_{-\infty}^{t} J(t_i)P_{ex}(t - t_i|t_i; J)dt_i. \tag{5}$$

[18] Then, differentiating with respect to time, and using the Leibniz rule (note that the dependence of P_{ex} and p_{ex} on J do not alter the differential relationship existing between the exceedance probability of T_{ex} and its pdf), we get

$$\frac{dS(t)}{dt} = J(t) - \int_{-\infty}^{t} J(t_i)p_{ex}(t - t_i|t_i; J)dt_i. \tag{6}$$

By comparing equations (3) and (6), the following expression for Q is then obtained:

$$Q(t) = \int_{-\infty}^{t} J(t_i)p_{ex}(t - t_i|t_i; J)dt_i, \tag{7}$$

which shows that the output flux can be expressed in terms of the input J and of the conditional exit time pdf. It is worth noticing that technically equation (7) is not a convolution, as the function $p_{ex}(t - t_i|t_i; J)$, which plays the role of a transfer function, depends on the whole sequence of input experienced by the system. In other words, because the system is nonlinear, an explicit definition of the transfer function in terms of the variables t and t_i alone is not possible. This automatically implies that the whole rainfall sequence contributes to define the exit time pdf of water.

[19] A key point is that the identity between the r.h.s. terms of equations (7) and (4) (i.e., $\int J(t_i)h(t - t_i)dt_i = \int J(t_i)p_{ex}(t - t_i|t_i; J)\, dt_i$) does not imply at all $h \equiv p_{ex}$. This evidence is clearly illustrated in Figure 2, where a graphical representation of equations (4) and (7) is provided during a 1 month sample time window which includes four pulse rainfall events (see the caption of Figure 2 for a more detailed comment). Mathematically, the difference between p_{ex} and h is explained by the time-variant nature of p_{ex}, and its nonlinear dependence on J. From a physical viewpoint, the difference between the hydrograph and the exit time pdf is instead related to the mixing and the displacement of old water during rainfall events. While the unit hydrograph quantifies the effect of a given event in terms of discharge, and is thus related to the speed at which the hydrologic signal propagates within a hillslope, the exit time distribution reflects the age of the runoff water and is controlled by pore water velocity and by mixing processes involving old and event water [see, e.g., *Beven*, 1989b, 2001]. Only when

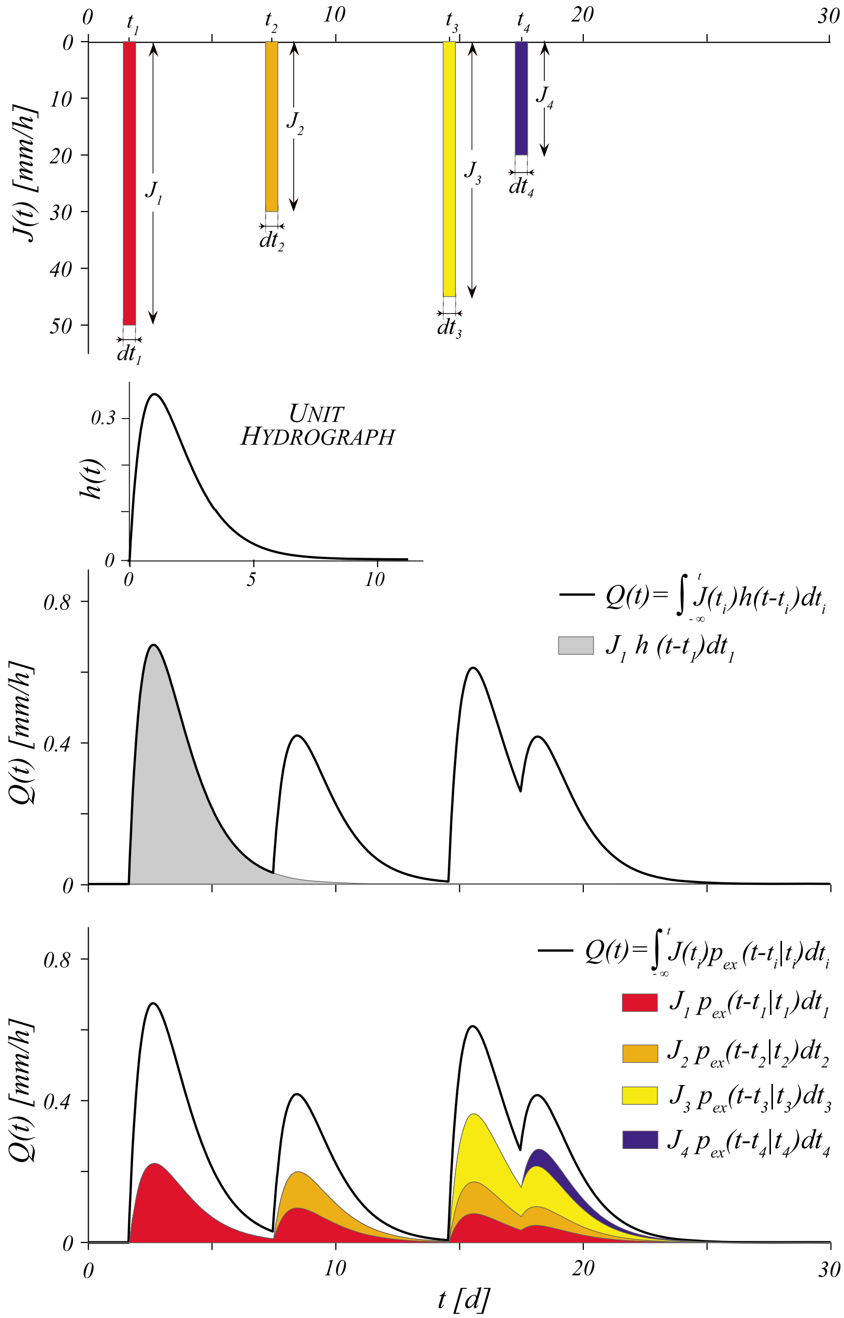

Figure 2. Difference between unit hydrograph and exit time pdf. (top) The temporal evolution of the rainfall input (four different pulses occurring at different times). Each pulse is represented by a different color. (middle) The discharge obtained using the traditional unit hydrograph approach (equation (4)) that does not distinguish the age structure of exiting particles (note that in this particular example we assume that losses are null and thereby the shaded area measures a volume equal to the corresponding rainfall volume $J(t_1)dt_1$). Also shown (inset) is the corresponding instantaneous unit hydrograph. (bottom) The same total discharge time series $Q(t)$ may be expressed as a convolution between the rainfall input and a set of time-variant exit time pdf's, once remobilization of old water is allowed. The temporal evolution of the contributions to Q due to water belonging to each of the four input pulses reported in Figure 2 (top) are represented by the shaded areas (which are coded by the same color of the corresponding input). Note that the white area in Figure 2 (bottom) represents water volumes whose exit time is larger than $t - t_1$.

the water storage before and after the event is null or, analogously, when there is no interaction between old and event water and the outflow corresponding to each event is composed only by water particles constituting the corresponding input event, p_{ex} and h would be the same. However, the commonly held belief that storm water is basically event water is nowadays considered a misconception [see, e.g., *Beven*, 2001], except for the special case of zero initial storage at the beginning of each event that might sometimes hold in arid catchments.

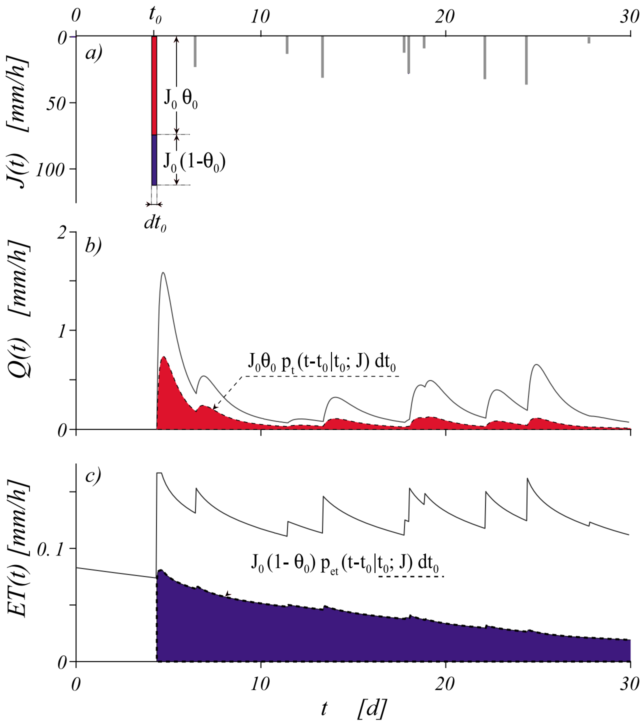

Figure 3. Time-variant conditional evapotranspiration and travel time pdf's. The color code indicates the instantaneous fractions of the total fluxes due to the rainfall pulse at time t_0. Note that subsequent events remobilize old (preevent) water.

[20] It is worth noting that the effectiveness of most linear rainfall-runoff schemes of the type shown by equation (4) (which are by definition unable to quantify the age of runoff) to reproduce observed hydrographs, suggests that the age of runoff can be indeed disregarded when the only focus is to reproduce the temporal evolution of runoff during floods. This stems from the fact that, at least to evaluate water flows, it is not vital to reproduce which particles are forced out of the control volume at a certain time during a given event, but only how many of them are released per unit time. The same considerations do not apply when considering the chemical composition of streamflows (i.e., the flux concentration of solute matter in hydrologic runoff), which primarily depends on the age of the water particles. Hence for solute fluxes a general operational relationship similar to equation (4) cannot be built.

3. A Lagrangian Description of Soil Moisture Dynamics: Travel and Evaporation Times Pdf's

[21] A theory that aims at properly describing the dependence of the exit time distribution on the full set of hydrological processes taking place within a catchment transport volume of the type shown in Figure 1, needs to account for the strongly nonlinear effects induced by evapotranspiration and soil moisture dynamics. To this end, we shall relax the assumption yielding $ET = 0$ and consider the whole soil moisture dynamics as described by equation (1). In such a case, by comparing equations (1) and (6), the following relation is obtained:

$$Q(t) + ET(t) = \int_{-\infty}^{t} J(t_i) p_{ex}(t - t_i|t_i; J) dt_i, \tag{8}$$

which expresses the overall output fluxes (evapotranspiration and discharge) in terms of the input J and of the conditional exit time pdf. To properly distinguish between the water particles undergoing evapotranspiration and the particles leaving V as discharge, we introduce the following definitions (Figure 1): (1) the travel time (T_t) is the time elapsed between the injection of the particle and the passage through the control section as discharge Q and (2) the evapotranspiration time (T_{et}) is the time elapsed between the injection and the release in the atmosphere as water vapor through the flux $ET(t)$. Hence, depending on the fate of a water particle, the exit time of each particle equals either its travel time (if the particle passes through the control section as water flow) or its evapotranspiration time (if the particle undergoes evapotranspiration)

$$T_{ex} = \begin{cases} T_t & \text{particles exiting as Q} \\ T_{et} & \text{particles exiting as ET.} \end{cases} \tag{9}$$

[22] According to this framework, the random nature of the variables T_t and T_{et} (inherent in their dependence on the spatial and temporal distribution of climate, soil and vegetation characteristics) will be described by looking at their conditional probability distribution functions, $p_t(t|t_i)$ and $p_{et}(t|t_i)$. In particular, to highlight the dependence of the conditional pdf's of T_t and T_{et} on the temporal evolution of the input rate, the notations $p_t(t|t_i; J)$ and $p_{et}(t|t_i; J)$ will be used. Accordingly, $p_t(t|t_i; J)dt$ represents the fraction of water particles injected in t_i whose travel time falls in the interval $[t, t + dt]$, and analogously for p_{et}. Figure 3 shows a typical evolution of ET and Q produced by a stochastic rainfall input J during a sample time period of 30 days: the contributions to Q and ET due to water particles injected at t_0 are represented by the shaded areas. The plots emphasize the dependence of conditional pdf's of T_t and T_{et} on the sequence of states experienced by the system, and the remobilization of old water induced by each rainfall event which renders the system highly nonlinear. Moreover, Figure 3b highlights once more the conceptual difference between the hydrograph response and the travel time pdf.

[23] Let $\theta(t_i)$ be the probability that a water particle injected at time t_i will not be transpired, that is, $\theta(t_i)$ and $(1 - \theta(t_i))$ are the fraction of water particles injected at t_i that exit V as Q and ET, respectively (see Figures 3b and 3c). Note that the value assumed by $\theta(t_i)$ depends on the whole hydrologic history of the system (i.e., $\theta(t_i)$ depends on the sequence of wet and dry periods after t_i, see Appendix B). According to equation (9), the exit time distribution is a linear combination of the travel and evapotranspiration time pdf's

$$p_{ex}(t|t_i; J) = \theta(t_i) p_t(t|t_i; J) + (1 - \theta(t_i))\, p_{et}(t|t_i; J). \tag{10}$$

[24] Note that if the evapotranspiration term is neglected (i.e., $\theta \equiv 1$), the exit time pdf p_{ex} coincides with the travel time pdf p_t. Otherwise, by inserting equation (10) into (8),

and separating the contributions due to discharge and evapotranspiration, we obtain

$$Q(t) = \int_{-\infty}^{t} J(t_i)\theta(t_i)p_t(t - t_i|t_i; J)dt_i \tag{11}$$

$$ET(t) = \int_{-\infty}^{t} J(t_i)(1 - \theta(t_i))p_{et}(t - t_i|t_i; J)dt_i. \tag{12}$$

[25] Equation (11) (equation (12)) expresses the discharge (the evapotranspiration rate) in terms of the input J and of the conditional travel (evapotranspiration) time pdf. The above equations generalize equation (7) when the partition between blue and green water (runoff and evapotranspiration) is accounted for.

4. Coupling Flow and Transport of Reactive and Passive Solutes

[26] The above scheme may be adopted to describe transport processes of reactive or conservative solutes in the hydrologic cycle. To this aim, we further assume that the solute concentration of the water particles inside V changes in time only in the case of reactive solutes, and that such concentration is not affected by the trajectories of the particles and thus by their position within V, a legitimate assumption when nonpoint sources and heterogeneous hydrologic media are considered [*Botter et al.*, 2005, 2009; *Rinaldo et al.*, 2006a, 2006b]. Under the above assumptions, the solute concentration C of the water particles stored in V at a given time t, depends only on the injection time t_i and (for reactive solutes) also on the time $t - t_i$ spent inside V by the particles (i.e., $C = C(t - t_i, t_i)$). The solute mass in storage within V at time t, $M(t)$, can be in this case expressed as

$$M(t) = \int_{-\infty}^{t} J(t_i)C(t - t_i, t_i)P_{ex}(t - t_i|J)dt_i. \tag{13}$$

[27] Deriving equation (13) with respect to t, one gets

$$\frac{dM(t)}{dt} = -\int_{-\infty}^{t} J(t_i)C(t - t_i, t_i)p_{ex}(t - t_i|t_i; J)dt_i + J(t)C_0(t) + \int_{-\infty}^{t} J(t_i)P_{ex}(t - t_i|t_i; J)\frac{dC(t - t_i, t_i)}{dt}dt_i. \tag{14}$$

[28] If we further assume that evapotranspiration processes do not change the solute concentration of the soil solution (i.e., plants incorporates the whole solution via passive uptake), the solute concentration C of the water particles stored in V, can be assumed to change through time only in response to possible chemical and/or physical mechanisms involving reactive solutes. This implies that the term $\left(\frac{dM}{dt}\right)_{react}$ in equation (2), which quantifies the rate of change of the solute storage due to physical and/or chemical reaction processes, can be expressed as

$$\left(\frac{dM}{dt}\right)_{react} = \int_{-\infty}^{t} J(t_i)P_{ex}(t - t_i|t_i; J)\frac{dC(t - t_i, t_i)}{dt}dt_i. \tag{15}$$

Inserting equation (15) into (2) and comparing the result with equation (13), we can express the solute mass flux exiting V at the time t as

$$\phi_Q(t) + \phi_E(t) = \int_{-\infty}^{t} J(t_i)C(t - t_i, t_i)p_{ex}(t - t_i|t_i; J)dt_i. \tag{16}$$

[29] We can split the output mass flux into the contributions specifically associated to ET and Q by using equation (10), and focus only on the mass flux associated with Q

$$\begin{aligned}\phi_Q(t) &= \int_{-\infty}^{t} J(t_i)\theta(t_i)C(t - t_i, t_i)p_t(t - t_i|t_i; J)dt_i \\ &= \int_{-\infty}^{t} \phi_0(t_i)\theta(t_i)\ell(t - t_i|t_i; J)dt_i,\end{aligned} \tag{17}$$

where $\ell(t|t_i) = C(t, t_i)p_t(t|t_i; J)/C_0(t_i)$ takes on the meaning of a lifetime distribution. Note that, for conservative solutes ($C(t - t_i, t_i) = C_0(t_i)$), the lifetime distribution ℓ coincides with the travel time distribution. Hence, the (conditional) travel time distribution of water, p_t, can be also defined as the solute mass flux produced at the outlet by a unit impulsive input of a passive conservative tracer.

[30] The above formulation generalizes previous mass response function approaches for solute transport [*Rinaldo and Marani*, 1987; *Rinaldo et al.*, 1989, 2006a, 2006b; *Botter et al.*, 2005], which were however based on a linear scheme analogous to that described by equation (4). Indeed, under the linearity and time invariance assumption, if we further assume that the initial storage is negligible (i.e., $p_t(t - t_i|t_i; J) = h(t - t_i)$) and focus on the propagation of the effective rainfall by neglecting evapotranspiration (i.e., $\theta(t) \equiv 1$), equation (17) becomes

$$\phi_Q(t) = \int_{-\infty}^{t} J(t_i)C(t - t_i, t_i)h(t - t_i)dt_i, \tag{18}$$

which is indeed the basic equation developed by *Rinaldo and Marani* [1987] and *Rinaldo et al.* [1989]. Note that in this formulation, the interaction between old and new water (which is not explicitly described through time-variant travel time pdf's) can be however included by introducing an additional reactive component superimposed to the flow (and possibly to biogeochemical processes), which mimics physical diffusion and mixing [see, e.g., *Botter et al.*, 2009].

5. Old Water Mobilization and Waiting Time Distributions

[31] In this section we provide a linkage between the travel time pdf and the hydrograph response, that will properly reflect the mobilization of old water (of different ages) in the response to an individual event. To this end we will focus for the moment only on the fraction of rainfall which propagates toward the outlet as streamflow ($\int_0^\infty J(x)\theta(x)dx$). Depending on the underlying soil moisture content, the movement of such particles in subsurface/groundwater environments can be relatively fast or extremely slow. In order to allow for analytical derivations, the dependence of such transport dynamics on the storage is conceptualized as follows. We assume that any single water particle in V can be characterized by one of the following complementary

states: (1) mobilized and (2) not mobilized. At any given time t, mobilized particles follow a hydrologic pathway destined to drive such particle out of V through the outlet as runoff Q even in the absence of future forcing rainfall events. The total flux of particle mobilized at time t will be denoted as $J_m(t)$. Conversely, not mobilized water particles are free to move within V but they are assumed not to exit through the control section in the absence of further rainfall events able to initiate their mobilization. This schematization is introduced to simplify the expressions for the exit time distribution, and helps the difference between the instantaneous unit hydrograph and the travel time distribution to be better visualized and understood, although it can be removed whenever appropriate (see section 8). Note also that we assume that the water particles cannot be transpired after their mobilization. The latter, however, seems to be a relatively mild assumption, as during rainfall events (when the soil is wet and the corresponding mobilization rates are expected to be significant) transpiration processes are extremely slow, while the transport processes taking place become relatively fast.

[32] The mobilization time (T_m) of a given particle is thus defined as the time at which the mobilization of such particle occurs, with respect to the time origin considered. In analogy with what seen before, T_m can be seen as a random variable whose pdf is determined by the temporal sequence of the water volumes rates mobilized by rainfall. Because T_m and T_i are not independent, the pdf of T_m conditional to a given injection time t_i, $p_m(t|t_i)$, should be considered. Obviously, $p_m(t|t_i)$ must be null for every $t < t_i$. Note that hereafter the dependence of the various pdf defining the transport features on the rainfall input J will be omitted to simplify the notation. Accordingly, let $P(T_m \geq t) = P_m(t|t_i)$ be the exceedance cumulative probability of the mobilization time, conditional to a given injection time t_i ($P_m(t|t_i) = 1 - \int_{t_i}^{t} p_m(x|t_i)dx$).

[33] By definition, the cumulative water volume mobilized in the time interval $(-\infty, t)$ is the time integral of the mobilization rate J_m from $-\infty$ to t. The same quantity can also be expressed as the sum of the contributions due to the various water pulses injected in V in the interval $(-\infty, t)$

$$\int_{-\infty}^{t} J_m(x)dx = \int_{-\infty}^{t} J(t_i)\theta(t_i)(1 - P_m(t|t_i))dt_i. \tag{19}$$

[34] Thus, differentiating equation (19) with respect to t (using the fact that $P_m(t|t) = 1$), we get

$$J_m(t) = \int_{-\infty}^{t} J(t_i)\theta(t_i)p_m(t|t_i)dt_i. \tag{20}$$

From the perspective of the age of runoff, it is assumed that every incoming water pulse can mobilize, besides part (or all) of the water particles constituting the pulse itself ('new water'), part of the water particles already stored in the control volume ('old water'). Hence, we define the waiting time (say T_w) as the difference between the time when the mobilization of a water particle occurs and the time in which the same water particle was injected into the control volume

$$T_w = T_m - T_i. \tag{21}$$

[35] Owing to the random nature of T_m, the waiting time is a random variable as well, which can be characterized probabilistically via its pdf ($p_w(t|t_i)$), conditional to the injection time t_i. As by definition we have

$$p_w(t - t_i|t_i) = p_m(t|t_i), \tag{22}$$

substituting back equation (22) into (20) we get:

$$J_m(t) = \int_{-\infty}^{t} J(t_i)\theta(t_i)p_w(t - t_i|t_i)dt_i, \tag{23}$$

which expresses the mobilization rate in terms of the overall rainfall and of the waiting time pdf. After the mobilization, each particle spends a certain amount of time inside V before reaching the outlet. The time elapsed from the mobilization of a water particle to its passage through the outlet (which is indicated as T_r) is assumed to be a random variable, whose pdf (h_r) is assumed to be time invariant for the sake of convenience. Accordingly, the discharge Q is expressed by the convolution between J_m and the response time pdf, h_r

$$Q(t) = \int_{-\infty}^{t} J_m(t_m)h_r(t - t_m)dt_m. \tag{24}$$

[36] The conditional travel time pdf, $p_t(t - t_i|t_i)$, can be thus expressed as a function of the conditional waiting time pdf and of the response time pdf by inserting equation (23) into (24), upon comparison with equation (11)

$$p_t(t - t_i|t_i) = p_w * h_r = \int_{t_i}^{t} p_w(t_m - t_i|t_i)h_r(t - t_m)dt_m, \tag{25}$$

where $*$ denotes the convolution operator. Equation (25) reflects the fact that the travel time of a water particle, T_t, is the sum of the waiting time T_w and of the response time T_r (i.e., $T_t = T_w + T_r$), where T_w and T_r are assumed as statistically independent random variables.

[37] In the above formulation, the mobilization of the water particles can be delayed with respect to the event responsible of producing their mobilization, a possible by-product of the finite speed at which hydrologic signals (e.g., spatial gradients of soil water content) can propagate within a hillslope [*Beven*, 2001]. However, if the delay time between the mobilization of the particles and the occurrence of the event initiating the mobilization is small compared to the overall travel time (see sections 6 and 7), at least for the computation of p_t, the mobilization rate $J_m(t)$ can be identified with the effective rainfall $J_e(t)$ (meant as the fraction of the actual precipitation producing an output at the outlet). Under the latter assumption, the pdf of the time spent from the mobilization to the exit represents the unit hydrograph, i.e., $h_r \equiv h$, and equation (25) becomes

$$p_t(t - t_i|t_i) = p_w * h = \int_{t_i}^{t} p_w(t_m - t_i|t_i)h(t - t_m)dt_m, \tag{26}$$

which represents a simplified linkage between travel time pdf, waiting time pdf and unit hydrograph.

[38] To make the interpretation of our analytical results easier, in what follows we shall assume that $J_m(t) \simeq J_e(t)$,

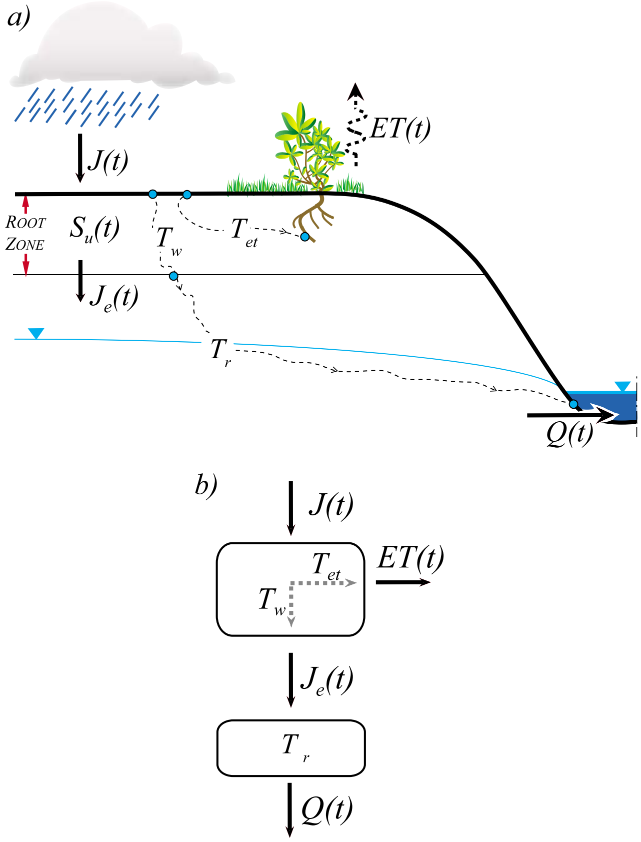

Figure 4. Physical and conceptual representations of the stochastic model for water mixing and transport within a hillslope. (a) Cross section of the transport volume reporting a schematic representation of the root zone and the groundwater regions and specifying the main components of the exit time, the waiting time (T_w) and the response time (T_r) for the particles that leave V as streamflow and the evapotranspiration time (T_{et}) for the particles undergoing evpotranspiration. Note that the hydrologic setting depicted here is purely indicative, provided that other morphologic configurations are equally plausible (see section 8). (b) Conceptual block diagram of the version of the model described in section 6. The upper soil region receives as input the overall rainfall, producing as output the evapotranspiration flux, ET, and the effective rainfall, J_e; the groundwater region, instead, transforms the effective rainfall into streamflows (Q).

and thus employ the more familiar notation of J_e and h to denote the mobilization rate and the response time pdf, respectively. Were this assumption relaxed, however, the paper conclusions would still remain valid.

[39] With the above premises, in the next section we will apply the above scheme by first specifying the mobilization rate as a function of the storage in the root zone, and then introducing mixing dynamics into the model as an additional component to the flow, as a way of predicting p_t and p_{ex}.

6. A Model for Water Mixing in Soil States

[40] To derive an analytical expression for the pdf's of T_w, T_t and T_{et}, we propose here a model that explicitly accounts for the partition of the output fluxes in green and blue water and for the mixing between old and new water occurring within the near surface soil layer. Even though in some cases other mixing processes (e.g., interactions and mixing with a permanent water table below the root zone; see *Beven* [2001] and section 8) can be equally important, mixing in the root zone represents a key process influencing the streamflow composition [*Maloszewski and Zuber*, 1982; *Maloszewski et al.*, 1992; *Weiler et al.*, 2003; *McGuire and McDonnell*, 2006; *Stumpp et al.*, 2009]. To model the above process, the overall soil water storage, $S(t)$, is split into two contributions (Figure 4): the contribution pertaining to the root zone (meant as a suitably defined near-surface soil region where soil moisture dynamics matters), $S_u(t)$; and a contribution pertaining to a subsurface-groundwater region, $S_g(t)$. While at any time $S = S_u + S_g$, the underlying mass conservation equations yields (see Figure 4)

$$\frac{dS_u(t)}{dt} = J(t) - J_e(S_u(t)) - ET(S_u(t)) \tag{27}$$

$$\frac{dS_g(t)}{dt} = J_e(S_u(t)) - Q(t). \tag{28}$$

[41] According to the above equations, the near-surface soil storage S_u receives as input the incoming rainfall J, while the corresponding losses are represented by evapotranspiration, ET, and deep percolation toward the deeper soil (or recharge), which would actually represent the mobilization rate J_m because of the fact that each groundwater recharge input is assumed to be transported to the outlet even in the absence of further inputs, but is denoted here as J_e according to the assumption discussion in section 5. In the specific case discussed here, the equivalence between J_m and J_e implicitly assumed in (27) and (28) is further justified by the highly nonlinear dependence of the percolation rate on the storage, which ensures a relatively rapid drainage from the root zone for relatively high soil moisture contents (see *Laio et al.* [2001] and *Rodriguez-Iturbe and Porporato* [2004], but see also section 7). Note also that the same assumption is commonly done by any threshold-based model of runoff production applied to the root zone [see, e.g., *Botter et al.*, 2007; *Porporato et al.*, 2004].

[42] In this example, the water particles percolating from the root zone are assumed to be advected and dispersed within the deep soil region as subsurface/groundwater flow without further mixing and interactions with other water particles characterized by different ages, until they eventually reach the outlet. According to the discussion provided in the previous section, the probability distribution of the time spent by the water particles percolating from the near-surface soil layer to the deeper region (i.e., from mobilization to the passage through the control section) defines in this case the unit hydrograph, h. Independently of the specific spatial configuration of the two regions chosen (e.g., Figure 4), the major assumptions here are that mobilized water particles do not contribute to the water storage that controls the evapotranspiration and the production of effective rainfall, and that no further mixing takes place after the mobilization. However, both these assumptions can be properly relaxed (section 8).

[43] The time spent in the upper region by a water particle, T_u, is a random variable. In particular, T_u is equal to the time to evapotranspiration (if at all the considered particle is transpired) or to the waiting time (if the particle is mobilized via percolation). Hence, in analogy with equation (10), the pdf of T_u conditional to a given injection time t_i, $p_u(t|t_i)$, can be expressed as

$$p_u(t|t_i) = \theta(t_i)p_w(t|t_i) + [1 - \theta(t_i)]\, p_{et}(t|t_i). \tag{29}$$

[44] Also, let $P_u(t|t_i)$ the cumulative probability of the time spent in the upper soil region conditional to a given t_i (i.e., $P_u(t|t_i) = 1 - \int_0^t p_u(x|t_i)dx$). As $dP_u(t|t_i)/dt = -p_u(t|t_i)$, using equation (29) we have

$$\frac{dP_u(t|t_i)}{dt} = -\theta(t_i)p_w(t|t_i) - [1 - \theta(t_i)]\, p_{et}(t|t_i). \tag{30}$$

To derive the waiting time distribution, some further assumptions are needed. A simple and reasonable hypothesis [*Botter et al.*, 2009] is to assume that the heterogeneity of the processes involved results, from the perspective of the age of the particles leaving the upper soil region, into an effectively well-mixed process (i.e., during evapotranspiration and mobilization the water particles that leave the system are randomly sampled among all the water particles contained in V). As shown in Appendix A, this translates in the following equations for the (conditional) mobilization and evapotranspiration time pdf's:

$$p_w(t - t_i|t_i) = \frac{J_e(t)P_u(t - t_i|t_i)}{\theta(t_i)S_u(t)} \tag{31}$$

$$p_{et}(t - t_i|t_i) = \frac{ET(t)P_u(t - t_i|t_i)}{[1 - \theta(t_i)]S_u(t)}. \tag{32}$$

[45] Thus, inserting equations (31) and (32) into (30), we get

$$\frac{dP_u(t - t_i|t_i)}{dt} = -(J_e(t) + ET(t))\,\frac{P_u(t - t_i|t_i)}{S_u(t)}, \tag{33}$$

which can be exactly integrated between t_i and t by imposing the initial condition $P_u(0|t_i) = 1$, leading to the following expression for the conditional exceedance probability of T_u:

$$P_u(t - t_i|t_i) = \exp\left(-\int_{t_i}^{t} \frac{J_e(x) + ET(x)}{S_u(x)}dx\right). \tag{34}$$

Hence, inserting equation (34) into (31), we get

$$p_w(t - t_i|t_i) = \frac{J_e(t)}{S_u(t)\theta(t_i)}\exp\left(-\int_{t_i}^{t} \frac{J_e(x) + ET(x)}{S_u(x)}dx\right). \tag{35}$$

[46] Using equations (35) and (25) the conditional travel time distribution can be expressed in terms of the fluxes and of the storage terms involved in the soil moisture balance as

$$\begin{aligned} p_t(t - t_i|t_i) &= \int_{t_i}^{t} p_w(t_m - t_i|t_i)h(t - t_m)dt_m \\ &= \int_{t_i}^{t} \frac{J_e(t_m)}{S_u(t_m)\theta(t_i)}\exp\left(-\int_{t_i}^{t_m} \frac{J_e(x) + ET(x)}{S_u(x)}dx\right)h(t - t_m)dt_m, \end{aligned} \tag{36}$$

where J_e, ET and S_u are derived by any hydrological model that solves equation (27) and θ can be expressed as a function of J_e, ET and S_u via equation (B2) (Appendix B).

[47] Reasoning in a similar manner, starting from equation (32), the following analytical expression of the evapotranspiration time pdf, p_{et}, can be obtained:

$$p_{et}(t - t_i|t_i) = \frac{ET(t)}{S_u(t)(1 - \theta(t_i))}\exp\left(-\int_{t_i}^{t} \frac{J_e(x) + ET(x)}{S_u(x)}dx\right). \tag{37}$$

Finally, the expression of the conditional exit time distribution, $p_{ex}(t_{ex}|t_i)$, can be obtained from equations (10), (35), (37) and (B2).

7. Numerical Simulations

[48] In this section, we analyze the waiting, travel, evapotranspiration and exit time pdf's emerging from a series of numerical Monte Carlo simulations of a simplified stochastic soil moisture model where the soil water content dynamics are driven by intermittent rainfall inputs. The simulations are based on the geomorphic setting and the mixing scheme described in section 6, which will be however analyzed and commented from the perspective of the general framework developed in the paper.

[49] The soil moisture model employed is similar to the classic point soil water balance model developed by *Rodriguez-Iturbe et al.* [1999] and *Laio et al.* [2001], a model already employed at catchment scales in numerous studies [e.g., *Porporato et al.*, 2004; *Settin et al.*, 2007; *Botter et al.*, 2007, 2008b, 2009]. According to the assumptions made in sections 2 to 6, the catchment is schematized as a single hillslope with area A, which is in turn subdivided into an upper soil region and a subsurface-groundwater region.

[50] The physical properties of the upper soil region (i.e., of the root zone) are described using constant (spatially averaged) parameters. In particular, the root zone is defined by specifying the root zone depth (i.e., the depth of the active soil layer), Z_r [L] and its porosity, n (dimensionless). The various terms defining the temporal evolution of the water volume stored in the root zone, $S_u(t)$, (see equation (27)) are modeled as follows:

[51] 1. $J(t)$, the rainfall rate, is first modeled at daily time scales as a point process, and is then disaggregated at subdaily time scales. Daily rainfall is conceptualized as a zero-dimensional marked Poisson process. The average frequency of wet days is $\lambda\,[T^{-1}]$, while daily rainfall depths are assumed to be exponentially distributed with mean α [L]. The daily rainfall is then disaggregated at time intervals of 45 minutes via multiplicative random cascades [e.g., *Gupta and Waymire*, 1993; *Molnar and Burlando*, 2005]. The production of surface runoff via infiltration excess is not allowed, while the production of surface runoff via saturation excess is neglected, though checking "a posteriori" that the occurrence of oversaturation events has a negligible probability in all the simulations performed.

[52] 2. $ET[s(t)]$, the evapotranspiration rate, is assumed to be linearly increasing with the relative soil water content $s(t) = S_u/(n\,Z_r\,A)$ from $ET = 0$ at the wilting point (for $s = s_w$) up to its maximum (potential) value ET_m at a suitable stress threshold (s*). Below s_w, ET is assumed to be null, while above s* evapotranspiration proceeds unrestricted ($ET = ET_m$).

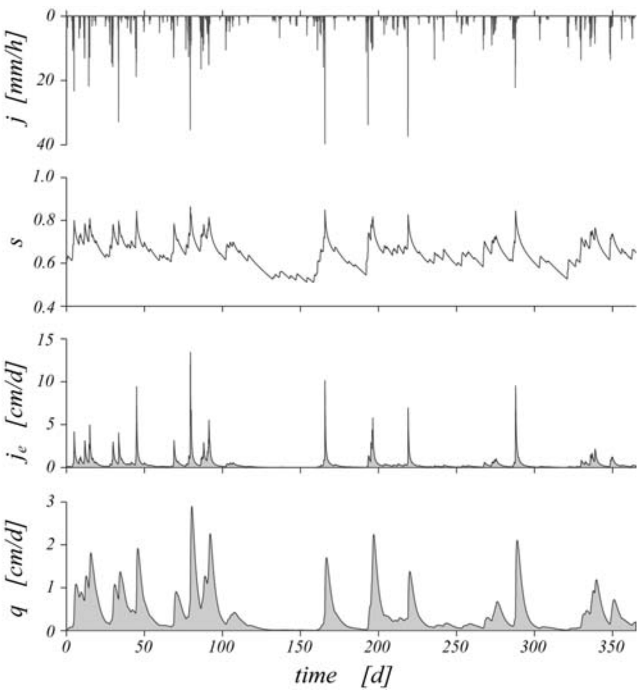

Figure 5. Complete numerical simulation of the model sketched in Figure 4. Temporal evolution of the following variables: input rainfall depths $j = J/A$ (synthetic data), (catchment averaged) relative soil moisture s, effective rainfall depths $j_e = J_e/A$, and specific (per unit area) discharge $q = Q/A$. The soil, vegetation, and transport parameters employed for this simulations are $n = 0.4$, $Z_r = 100$ cm, $s_w = 0.2$, $s^* = 0.45$, $K_{sat} = 50$ mm/h, $c = 15$, $ET_{\max} = 0.25$ cm/d, $k = 0.5$ d^{-1}, $\lambda = 0.3$ d^{-1}, and $\alpha = 20$ mm.

The parameters s_w, s^* and ET_m are assumed to be representative for the evapotranspiration process occurring in the considered basin during a given season.

[53] 3. According to a widely employed parametrization of the vertical flow driven by gravity (see, e.g., *Rodriguez-Iturbe et al.* [1999] and *Rodriguez-Iturbe and Porporato* [2004] for a review), the effective rainfall (or deep percolation rate) $J_e[s(t)]$ is assumed to be proportional to a given power of the relative soil water content s ($J_e \propto s^c$), where the proportionality constant depends on the saturated hydraulic conductivity K_{sat} [see, e.g., *Laio et al.*, 2001; *Settin et al.*, 2007]. Though being practically equivalent to any threshold-based scheme that assumes the existence of a field capacity, this schematization is more convenient from a computational point of view.

[54] In the numerical simulations, according to the theoretical approach described above, when an effective rainfall pulse is released from the upper soil it is then propagated toward the outlet as subsurface/groundwater flow [e.g., *Botter et al.*, 2007]. The groundwater region in this case acts as a single linear reservoir, and the instantaneous unit hydrograph that describes the subsurface/groundwater response is an exponential function with parameter k [T^{-1}], the inverse of the mean response time characterizing the subsurface region. Note that according to the lumped nature of the model and to the assumed statistical stationarity of the hydrologic and ecologic processes taking place, all the parameter values are assumed to be spatially and temporally averaged values. In other words, intra-annual variations of climatic and vegetation conditions are neglected [see *Porporato et al.*, 2004; *Settin et al.*, 2007; *Botter et al.*, 2007].

[55] Figure 5 shows the temporal evolution of some key hydrologic variables deriving from the application of the soil moisture and hydrologic models described above. In particular, Figure 5 plots the evolution of the rainfall depths ($J(t)/A$), of the normalized soil moisture, ($s(t) = S_u(t)/(An\,Z_r)$), of the effective rainfall depths ($J_e(t)/A$), and of the normalized streamflows ($Q(t)/A$) during a sample time window of 1 year. The hydrologic parameters used are reported in the caption of Figure 5. Figure 5 highlights the intermittency of the rainfall forcing and the stochastic variability of the soil water content, which is clearly reflected also by the streamflow fluctuations.

[56] The numerical solution of the water balance model during a relatively long time period provides the basic ingredients to evaluate how the waiting time pdf's in the upper soil layer depends on the underlying soil-moisture dynamics. Our tenet is that the intensity of the input-output fluxes forcing the catchment must affect significantly the time scale of the water renewal time in hillslopes. From an analytical viewpoint, the control exerted by the climate and the related ecohydrologcal processes on the ensuing transport mechanisms (at least for the specific mixing scheme considered in this paper) is mediated by the terms J_e, ET, S_u and θ (see equation (35)), which depend on soil, vegetation and climate features. In particular, we will focus here on the effect induced by rainfall properties, which is arguably one of the most important controls on the mixing exerted by the root zone.

[57] Figure 6 explores the dependence of the water renewal time in a hillslope on the underlying climatic features of the catchment. In particular, Figure 6a shows the (steady state) mean waiting time ($\langle T_w \rangle$) for the water particles injected within V during 1000 years of Monte-Carlo simulation of the soil moisture model, as a function of the following dimensionless factors: the ratio between the mean rainfall depth and the effective soil depth, $\alpha/(nZ_r)$, and the ratio between the rainfall frequency and the normalized maximum evapotranspiration depth, $\lambda\, n\, Z_r/ET_m$. The graph has been obtained by varying the rainfall frequency and the mean rainfall rate, and keeping the other parameters as constants. The plot clearly indicates that, as expected, in wet climates the mean waiting time is smaller than that observed in dry climate conditions because of the relatively high intensity of the input flux, which determines the increasing of the frequency of mobilization episodes (runoff events). The graph also suggests that the mean waiting times resulting from the mixing scheme developed (at least in the range of climatic conditions explored) is of the order of some 100s of days, a value quite compatible with the mean travel time estimates suggested by many experimental and theoretical studies proposed in the literature [e.g., *Rodhe et al.*, 1996; *McGuire et al.*, 2002]. Figure 6b shows a semilog plot of two sample conditional waiting time pdf's obtained under two different climatic regimes: a "dry" regime ($\lambda = 0.1$ d^{-1} and $\alpha = 0.5$ cm, point A in Figure 6a) and a "wet" regime ($\lambda = 0.3$ d^{-1} and $\alpha = 2$ cm, point B in Figure 6a). The conditional waiting time pdf's reported in the graph clearly emphasizes the relatively long waiting times characterizing the dry climate regime, as well as the dependence of the high-frequency fluctuations of p_w on the injection time (and

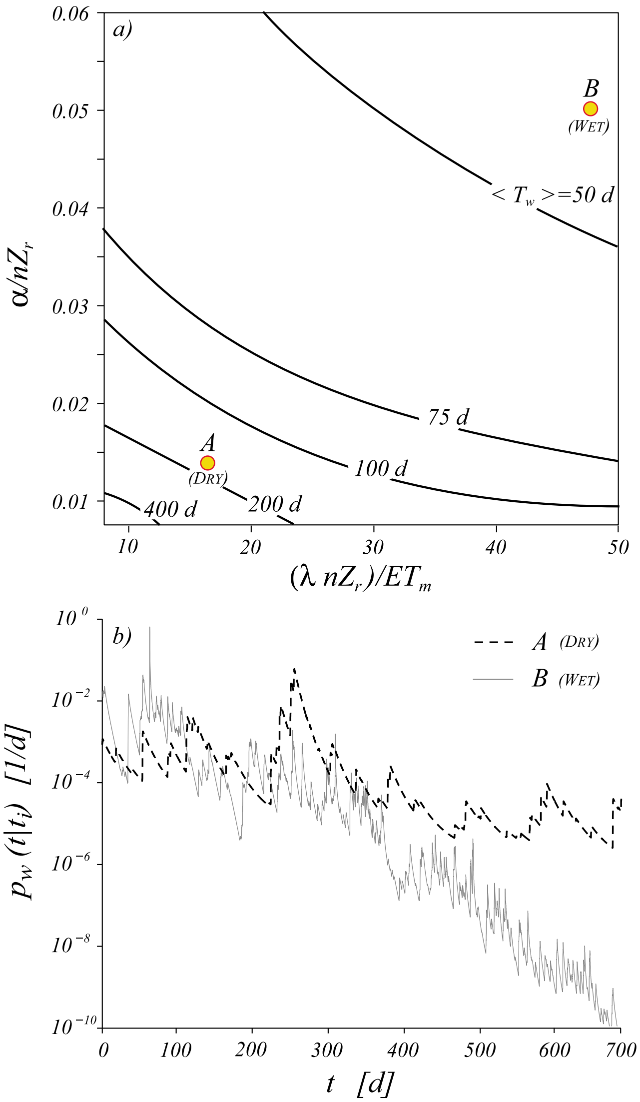

Figure 6. (a) Expected value of the waiting times ($\langle T_w \rangle$) for water particles injected during 1000 years of Monte-Carlo simulations in control volume V shown in Figure 4, as a function of the ratio between the mean rainfall depth and the effective soil depth, $\alpha/(nZ_r)$, and of the ratio between the rainfall frequency and the normalized maximum evapotranspiration depth, $\lambda\ n\ Z_r/ET_m$. The mean waiting times emerging from the mixing scheme (in the range of climatic conditions explored herein) is typically of the order of 100s of days. (b) Conditional waiting time pdf's corresponding to two different climatic conditions, a dry climate regime ($\lambda = 0.1$ d^{-1} and $\alpha = 0.5$ cm, point A in Figure 6a) and a wet climate regime ($\lambda = 0.3$ d^{-1} and $\alpha = 2$ cm, point B in Figure 6a). The other parameters are the same as used in Figure 5.

thus on the specific sequence of rainfall pulses determining the mobilization of the water particles stored in V), induced by the stochasticity of rainfall patterns.

[58] Figure 7 investigates the effect of rainfall properties on the features of the travel time distribution, by plotting (1) the conditional waiting time pdf, (2) the instantaneous unit hydrograph, and (3) the conditional travel time pdf (i.e., the convolution between the two) under the regimes highlighted in Figure 6. In particular, in the example reported in Figure 7 we assume an exponential instantaneous unit hydrograph with a mean response time of 2 days (a value which can be considered representative of the basic time scale of the subsurface hydrologic response in relatively small catchments of the type we are interested herein). The semilog plots show that, particularly under dry climate conditions, both the mean and the tail of the travel time distribution are largely controlled by the underlying waiting time pdf (i.e., $T_t \simeq T_w \gg T_r$). Meanwhile, the insets evidence that the travel time pdf is somewhat smoother than the corresponding waiting time pdf, particularly for small t, due to the dispersive effect induced by the transport features occurring in the deeper soil region. Nevertheless, the overall difference between p_w and p_t appears to be relatively small in all the cases investigated. Of course, this fact cannot be generalized as it may be a byproduct of the specific values assumed for the mean response times in

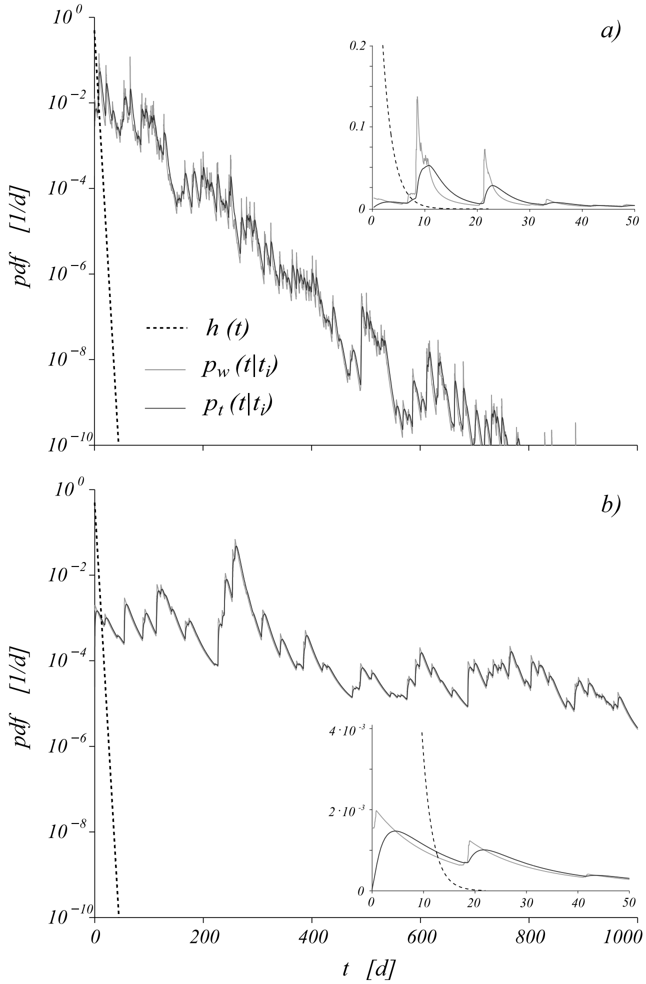

Figure 7. Conditional travel time distribution resulting from the convolution between the waiting time pdf and the instantaneous unit hydrograph under the two different climatic regimes explored in Figure 6. The semilog plots show that particularly under dry climate conditions the mean and the tail of the travel time distribution are controlled by the waiting time distribution (i.e., $T_t \simeq T_w \gg T_r$). The normal plot shown in the insets, instead, evidences that the travel time pdf is smoother than the corresponding waiting time pdf. All the parameters are the same as used in Figure 6.

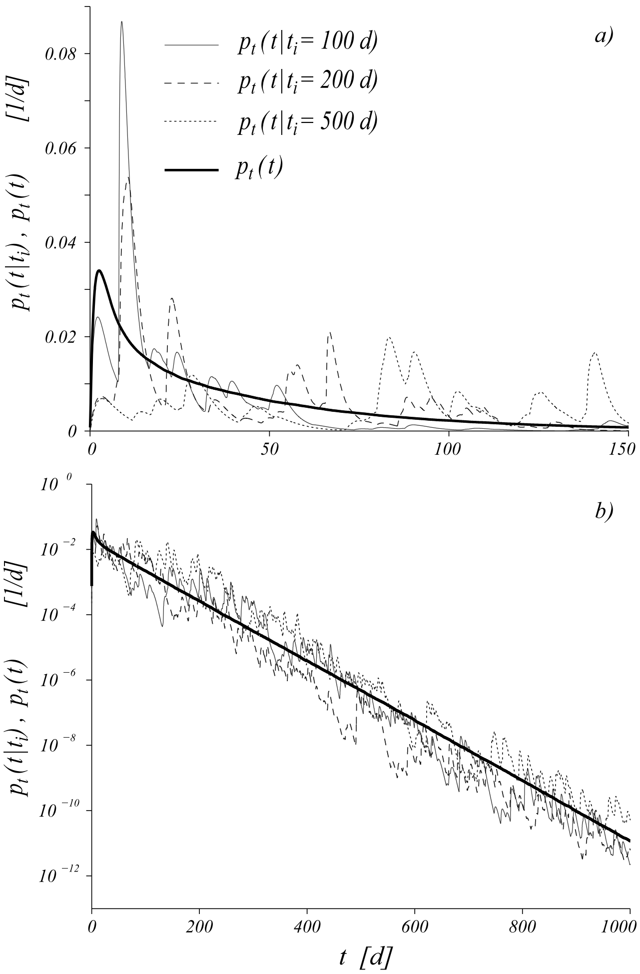

Figure 8. (a) A set of conditional travel time pdf's, $p_t(t|t_i)$, corresponding to three different injection times obtained from the numerical simulations performed under the wet climate regime. The marginal travel time distribution obtained by averaging the conditional travel time pdf's is also shown. (b) Same as Figure 8a but in a semilog plot. The graph emphasizes that the long-term decay of the individual conditional travel time pdf's is similar to the decay of the marginal distribution. All the model parameters are the same as used in Figure 6a.

these simulations, whereas it does also depend on the specific mixing scheme employed. A touch of generality emerges, however. In fact, the mixing between old and new water during rainfall events is likely to be the main reason behind the disparity frequently observed in the field between the mean travel time estimated from the analysis of the chemical composition of the streamflows ($O(10^2)$ [d]), and the mean response time derived from the calibration of event-based rainfall-runoff models ($O(10^0)/O(10^1)$ [d]) [e.g., *McDonnell et al.*, 1991; *Rodhe et al.*, 1996; *McGuire et al.*, 2002, 2007; *Rinaldo et al.*, 2006b; *Fiori and Russo*, 2008]. The dominant role of the waiting time in determining the water and solute travel time of stream waters could also explain the observed independence of the mean travel time on the catchment size [e.g., *McGlynn et al.*, 2003]. Indeed, while $\langle T_r \rangle$ is expected to depend on the catchment area due to the variability of the drainage density with the spatial scale, the mean waiting time $\langle T_w \rangle$ should be arguably independent on the catchment area.

[59] A rather important issue in the hydrological literature concerns the time variance of the travel time distribution (meant as the variability of the shape of the travel time pdf's characterizing the various pulses constituting the input). Indeed, postulating the long-term stationarity of the flow field allows the relationship between input and output concentrations to be considerably simplified [*Niemi*, 1977]. For this reason, the time invariance of travel time distributions has been frequently postulated in the literature. Numerical and analytical results have suggested the applicability of such an assumption to quite different hydrologic systems [e.g., *McDonnell*, 1990; *Nyberg et al.*, 1999], particularly when the time is substituted by a flow corrected time to compensate nonstationary unsteady flow fields (which is however a legitimate operation only when the overall volume of the storage remains approximately constant) [*Niemi*, 1977; *Maloszewski and Zuber*, 1982; *Rodhe et al.*, 1996; *Fiori and Russo*, 2008; *Russo and Fiori*, 2009]. The time invariance assumption, however, seems to be partially at odds with the high degree of intermittency exhibited by the rainfall forcing. Figure 8a shows a set of conditional travel time pdf's $p_t(t|t_i)$ corresponding to three different injection times t_i resulting from the numerical Monte Carlo simulations performed under wet climate conditions in the examples of Figures 5 and 6. Figure 8a also shows the marginal travel time distributions obtained by properly averaging the conditional travel time pdf's according to Bayes' rule (see equation (38) for a rigorous definition of the marginal pdf).

[60] The plot clearly indicates that for relatively small t, all conditional travel time pdf's $p_t(t|t_i)$ are quite different among each other, and all differ considerably from the marginal travel time pdf p_t. The semilog plot of Figure 8b, however, evidences that the long-term behavior of the individual conditional travel time pdf's tend to approximate well the marginal distribution. The mean of the conditional travel time pdf does not exhibit a marked variability when different injection times are considered. This notable feature is due to the fact that, because of the age mixing taking place in the root zone, in the long run the fluctuations produced by the stochasticity of the climate forcings become progressively less important, and the long-term decay of the travel time pdf chiefly depends on the average rainfall, soil and climate conditions. These results suggest that the steady state approximation is in general unreliable when considering short-term features of the system responses, but may be a valid assumption (particularly under wet climate regimes) if one focuses on the long-term behavior of the catchment. The impact of the interannual variability of the climatic and rainfall features on such results, and their dependence on the specific mixing scheme adopted still remain to be assessed.

[61] Figure 9 investigates the differences among the marginal travel time ($p_t(t)$), evapotranspiration time ($p_{et}(t)$) and exit time ($p_{ex}(t)$) pdf's under the reference wet (Figure 9a) and dry (Figure 9b) climatic regimes described by Figure 6. The above marginal distributions can be calculated by suitably averaging the corresponding conditional pdf's according to Bayes' rule, i.e.,

$$p_{t,et,ex}(t) = \frac{1}{\int_0^\infty J(x)dx} \int_0^\infty p_{t,et,ex}(t|t_i)\, J(t_i)dt_i. \qquad (38)$$

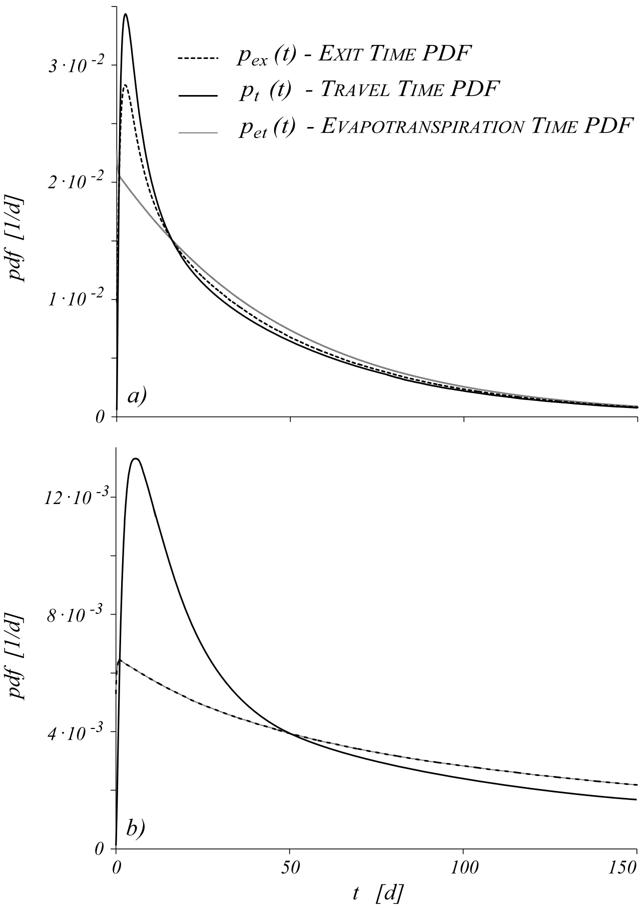

Figure 9. Marginal exit time (dashed line), travel time (solid black line) and evapotranspiration time (solid grey line) pdf's under the different climatic conditions indicated in Figure 6: (a) dry climate and (b) wet climate. All the model parameters are the same as used in Figure 6.

[62] Note that even though each conditional exit time pdf is a linear combination of the corresponding (conditional) travel time and evapotranspiration time pdf's (see, e.g., equation (10)), the same result does not apply to the marginal pdf's because the function θ varies with the injection time t_i. In most cases, however, the temporal variability of θ around its mean value is relatively weak, and the marginal exit time distribution results to be relatively well approximated by the linear combination of the travel and evapotranspiration time pdf's, as clearly shown by Figure 9. In particular, Figure 9a shows that in the wet regime the evapotranspiration time pdf has a smaller mode, a weakly larger mean, and a heavier tail with respect to the travel time pdf. The slight difference between the mean evapotranspiration time pdf and the travel time pdf is explained by the high efficiency of the transpiration processes ensured by relatively high soil moisture contents. The exit time pdf is in between the two curves representing the travel time and the evapotranspiration time pdf, reflecting the fact that the mean value of θ is close to 0.4. The three curves, however, tend to coincide for large times. Figure 9b shows that in the dry regime the evapotranspiration time has a fat tail, leading to a mean evapotranspiration time much larger than the mean travel time. This is due to the low efficiency of the transpiration process induced by vegetation water stress (a key phenomenon in dry catchments). In this case, however, the exit time pdf is practically coincident with the evapotranspiration time pdf, because of the extremely small values of θ resulting from the soil water balance model implying that most of the water particles entering dry catchments undergoes transpiration.

[63] The last numerical simulation discussed in this paper concerns the transport of a non reactive solute in the hydrologic response, an application which can be considered the end product of the model developed. The solute is assumed to be introduced into the control volume dissolved into rainfall. In particular, the solute rainfall concentration $C_0(t)$ is assumed to be the sum of a colored noise, superimposed to a sinusoidal drift with an amplitude equal to the mean input concentration, and a period of year. The solute is assumed to be passively transpired by plants and it is released toward the channel dissolved in the streamflows at a rate ϕ_Q according to equation (17) with $C(t - t_i, t_i) = C_0(t_i)$. The output flux concentration is then computed (for both the dry and the wet climate regimes) as the ratio between ϕ_Q and Q. In the plot shown in Figure 10a, the input and the output concentrations, normalized by the average input concentration $\langle C_0 \rangle$, are reported for a sample time window of 5 years. The graph shows that the fluctuations of the input are strongly damped in the output signal as a result of the mobilization and release of water particles with different ages (a key effect already evidenced by, e.g., *McGuire and McDonnell* [2006]). The graph also suggests that the damping effect is more pronounced for dry climates because the memory of the system is longer due to the relatively small frequency of runoff events and the integration effect exerted by the watershed becomes more effective. The average age of the water particles stored within V released from the control volume as streamflow is larger in dry climates because of the relatively large water renewal times in the root zone.

[64] We finally note that our tools are ideally suited to study the reliability of travel time pdf estimates based on time-invariant schemes, the relation between solute and water loads under different integration time scales, and the impact of climate soil and vegetation features on the resulting average flux concentrations of streamflows [e.g., *Rinaldo and Marani*, 1987; *Evans and Davies*, 1998; *Gupta and Cvetkovic*, 2000, 2002; *Baresel and Destouni*, 2005, 2006; *Lindgren et al.*, 2004; *Godsey et al.*, 2009].

8. Discussion

[65] The general time-variant nature of the travel time distribution and its explicit dependence on the various ecohydrologic processes taking place in soil states has been derived from mass conservation without the aid of specific assumptions (sections 2, 3 and 4). Exploring the dependence of the travel time pdf on climatic and ecohydrologic attributes, instead, further requires the specification of the geomorphic setting (e.g., the two-layer scheme shown in Figure 4, equations (27) and (28)) and of the nature of the mixing processes involved (where and how water mixes, see section 6). It should be emphasized, however, that the case discussed in sections 6 and 7 (and the specific mobilization scheme and the geomorphic setting employed therein) represent just one of the possible applications of the model.

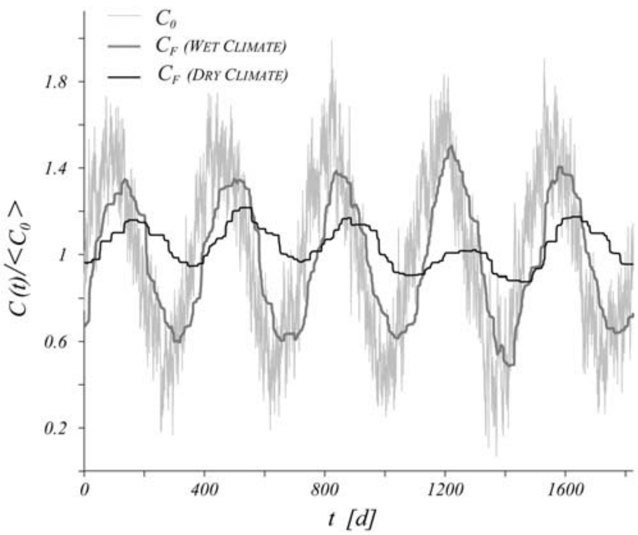

Figure 10. Temporal evolution of the input $C_0(t)$ and output $C_F(t) = \phi_Q(t)/Q(t)$ flux concentrations corresponding to the numerical simulation of the transport and flow models described in the paper during a sample time window of 5 years. Concentrations are normalized by the average input concentration $\langle C_0 \rangle$. The output flux concentrations are shown both for the dry and the wet reference climate regimes explored in the paper. All the model parameters are the same as used in Figure 6.

[66] In fact, the proposed generalization of Taylor's theorem to describe partition functions for different fluxes, including in particular evapotranspiration as a byproduct of soil moisture dynamics, applies without restrictions on the nature of control volumes or hydrologic processes included in the model. In what follows, we provide a few examples by addressing the following cases: (1) the case when the system geometry is further simplified and a single control volume is considered, (2) the case where groundwater mixing processes are included in the formulation, and (3) the case when the mixing mechanisms in hillslopes must be modeled according to a scheme other than that described in Appendix A.

[67] In our first example, the hillslope/catchment is described as a simple dynamical system defined by a single control volume [*Kirchner*, 2009], where a constitutive relation between outflowing discharge Q and total catchment storage $S(t)$ (i.e., $Q(S(t))$) can be established. The basic equations in this case then read

$$\frac{dS(t)}{dt} = J(t) - Q(t) - ET(t) \tag{39}$$

$$Q(t) = a\; S(t)^b, \tag{40}$$

where a, b are parameters, possibly obtained from a suitable recession analysis [e.g., *Brutsaert and Nieber*, 1977]. Under the mixing assumption described in Appendix A, according to which the water particles are randomly sampled among all the available particles, the travel time distribution can be in this case expressed by an equation similar to equation (35), with J_e replaced by Q

$$p_t(t-t_i|t_i) = \frac{Q(t)}{S(t)}\,\frac{e^{-\int_{t_i}^{t}\frac{Q(x)+ET(x)}{S(x)}dx}}{\theta(t_i)} \tag{41}$$

and where the partition function θ is

$$\theta(t_i) = \int_{t_i}^{\infty}\frac{Q(\tau)}{S(\tau)}e^{\int_{t_i}^{\tau}\frac{Q(x)+ET(x)}{S(x)}dx}d\tau. \tag{42}$$

[68] Note that the linear (time invariant) reservoir scheme for travel times widely employed in hydrology is recovered for $ET(t) = 0$ (hence $\theta \equiv 1$) and $b = 1$. Indeed $Q(t) = a\; S(t)$ yields $p_t = ae^{-a(t-t_i)}$ in equation (41). Note that also in this simplified case, only the direct measurement of all relevant fluxes would allow a proper determination of the travel time pdf. This version of the model could be seen as a particular case of the mobilization model presented in section 6, where the lower state would transfer instantaneously the recharge from the upper state to the outlet.

[69] A further elaboration of the proposed framework deals with alternative mixing schemes. In the paper we have focused on the mixing taking place in the root zone, which involves rainfall and soil moisture (a process that is deemed central for the determination of the travel times, except for particular cases). However, the more involved case where mixing occurs both in the root zone and in the groundwater region (see Figure 4) is amenable to analytical solution as well. In such a case, with respect to the notation used in section 6, one would obtain a time variant (conditional) distribution of the time spent in the groundwater region, say $p_g(t|t_m)$ (where the time t_m indicates the time when mobilization from the root zone to the saturated groundwater flow has occurred). In this case the mass balance equations are still (26) and (27), and the expression of the waiting time pdf in the root zone in the same provided in section 6. However, the further mixing in the groundwater region allows for some of the water particles reaching the groundwater during a given event to be trapped therein until the occurrence of a subsequent event able to push them out of V. If the mobilization scheme described in Appendix A is assumed to hold also in the groundwater region (and the probability of being pushed out of the control volume for the particles with a given age is proportional to the relative abundance of stored particles with that age), the pdf of the times spent in the groundwater is

$$p_g(t-t_m|t_m) = \frac{Q(t)}{S_g(t)}\; e^{-\int_{t_m}^{t}\frac{Q(x)}{S_g(x)}dx}, \tag{43}$$

while the travel time pdf is given by the convolution between p_w and p_g

$$p_t(t-t_i|t_i) = \int_{t_i}^{t} p_w(t_m - t_i|t_i)p_g(t-t_m|t_m)dt_m, \tag{44}$$

with the symbols' notation of section 6. Whether the mixing processes in groundwater may be important to define the overall travel time pdf in catchments or not, still remains to be assessed.

[70] All the above examples assume that mobilization of water particles from a hillslope is a neutral process from the perspective of their age because water particles are randomly drawn from the whole storage. Such a simple scheme, whose physical basis is discussed in Appendix A, has been adopted because it is a reasonable compromise that embeds the simultaneous effect of macropores and downslope age distributions, still allowing analytical solutions. Nevertheless, other mixing schemes may be numerically tackled and easily included in the proposed framework. Among these we mention (1) piston flow like models producing the preferential release of old water, (2) preferential flowpath models leading to the preferential expulsion of new water [see, e.g., *Botter et al.*, 2009], and (3) complex threshold-based schemes, where the percentage of new/old water released during a given event depends on the actual soil water content and the underlying hydrologic conditions. Needless to say, only the comparison with tracer field data would allow an objective evaluation of the reliability and the robustness of the above mentioned schemes.

9. Conclusions

[71] The following conclusions are worth mentioning:

[72] 1. A general framework based on the Lagrangian formulation of transport has been formulated which, moving from well established linear schemes of the hydrologic response, has provided a general quantitative linkage between the rainfall forcing and the output fluxes in catchments seen as nonlinear systems with memory. We suggested that the whole sequence of ecohydrological processes taking place in the soil (epitomized by the underlying soil moisture dynamics) affects the travel time distribution of water and conservative solutes in river basins, due to the pronounced nonlinearity of the system, and the memory it retains of the hydrologic history. All the above considerations possibly put into question the paradigm upon which the isotope hydrology is based. In fact, the variant nature of the travel times prevent but an average determination of travel times from observations where isotope dating occurs only for rainfall and runoff. Depending on cases, the average determination over all initial times may or may not be significant as fluctuations may be dominant in certain conditions.

[73] 2. The distinction between unit hydrographs and travel time distributions has been addressed and discussed. Moreover, a suitable conceptualization of the runoff production mechanisms shows the relation existing between the instantaneous unit hydrograph and the travel time pdf, which is quantified via a set of time variant waiting time pdf's expressing the age of the effective rainfall.

[74] 3. A model for the water mixing taking place in catchment soils (here referred to as root zone for the nature of the example chosen but not necessarily confined to it) has allowed the travel time pdf to be expressed analytically in terms of the underlying soil moisture dynamics. The specific scheme developed, which is neutral from the perspective of the water age because it assumes that the production of effective rainfall involves at random all the available ages, mimics the mixing processes between old and new water that are likely to occur in the soil during flushing episodes triggered by floods. Mean travel times emerging from this scheme are in accord with the range of values found experimentally in the literature. The conditional and time-variant nature of the travel time distributions is also documented with specific examples based on numerical simulations.

[75] 4. The analytical relationship derived and the numerical simulations performed suggest that, particularly in dry climate regimes, the mixing dynamics taking place in the soil state and the intermittency of rainfall are key factors to determine the shape of observed travel time pdf's.

[76] 5. A transport study of passive solute in this framework emphasizes the differences that climatic conditions produce on flux concentrations in the runoff, and the influence of the underlying climate conditions on the dampening of the input chemical signal.

Appendix A: Derivation of Equations (31) and (32)

[77] To derive the conditional pdf's of T_w and T_{et} we assume that heterogeneity and randomness of the processes involved (infiltration, preferential flow paths, capillary raise, root distribution) results, from the perspective of the age of the particles leaving the upper soil region via deep percolation and evapotranspiration, in a neutral (or well mixed) process (i.e., during the evapotranspiration and the mobilization processes, the water particles that leave the system are randomly sampled among all the water particles in the system). This is tantamount to assuming that the relative fraction of water particles mobilized (or evapotranspired) at a given time instant t that are characterized by a given injection time t_i is equal to the relative fraction of water particles contained at the time t in the upper soil region, characterized by that injection time. In mathematical terms

$$\frac{J(t_i)\theta(t_i)p_w(t-t_i|t_i)}{J_e(t)} = \frac{J(t_i)P_u(t-t_i|t_i)}{S_u(t)} \tag{A1}$$

$$\frac{J(t_i)[1-\theta(t_i)]p_{et}(t-t_i|t_i)}{ET(t)} = \frac{J(t_i)P_u(t-t_i|t_i)}{S_u(t)}. \tag{A2}$$

[78] The left-hand side of equations (A1) (of equation (A2)) indeed expresses the relative contribution to the effective rainfall rate (to the evapotranspiration rate) evaluated at time t which is due to water particles injected in V at time t_i, normalized by the overall effective rainfall rate (evapotranspiration rate) at time t. The right-hand side of these equations, instead, represent the relative contribution to the storage in the upper soil layer ($S_u(t)$) due to water particles injected in t_i (normalized in this case by the overall storage at that time). Isolating $p_w(t - t_i|t_i)$ and $p_{et}(t - t_i|t_i)$ from equations (A1) and (A2), equations (31) and (32) are straightforwardly obtained.

Appendix B: Derivation of the Function $\theta(t)$

[79] The imposition of the normalization condition to the conditional waiting time pdf, i.e.,

$$\int_0^\infty p_w(\tau|t_i)d\tau = 1 \tag{B1}$$

translates into an analytical expression of the function $\theta(t_i)$ (defining the fraction of water particles injected inside V at time t_i which are destined to exit V as streamflow). In particular, by inserting equation (35) into equation (B1), and isolating $\theta(t_i)$, we have

$$\theta(t_i) = \int_{t_i}^{\infty} \frac{J_e(t_m)}{S_u(t_m)} \exp\left[-\int_{t_i}^{t_m} \frac{J_e(x) + ET(x)}{S_m(x)} dx\right] dt_m, \quad \text{(B2)}$$

which expresses θ in terms of ET, J_e and S_u. Equation (B2) highlights that the value of θ at a given time t_i depends on the sequence of states experienced by the system after t_i, reinforcing the fact that the system is highly nonlinear.

[80] **Acknowledgments.** This research is funded by ERC Advanced grant RINEC 22761. Support from the Research Project RIMOF2 (Fondazione Cassa di Risparmio di Verona, Vicenza, Belluno e Ancona) and the research project MIUR-PRIN 2008 (Analisi dei processi di flusso e trasporto di inquinanti a scala di versante) is also acknowledged. The authors wish to thank Keith Beven, University of Lancaster, for his insightful review of a draft of the manuscript and contribution to the final presentation of section 2. Two anonymous reviewers have also provided useful suggestions.

References

Baresel, C., and G. Destouni (2005), Novel quantification of coupled natural and cross-sectoral water and nutrient/pollutant flows for environmental management, *Environ. Sci. Technol.*, *39*, 6182–6190.

Baresel, C., and G. Destouni (2006), Estimating subsurface nitrogen accumulation-depletion in catchments by input-output flow analysis, *Phys. Chem. Earth*, *31*, 1030–1037.

Beven, K. (1981), Kinematic subsurface stormflow, *Water Resour. Res.*, *17*(5), 1419–1424.

Beven, K., and P. Germann (1982), Macropores and water-flow in soils, *Water Resour. Res.*, *18*(5), 1311–1325.

Beven, K. J. (1989a), Changing ideas in hydrology: The case of physically based models, *J. Hydrol.*, *105*, 157–172.

Beven, K. J. (1989b), *Interflow*, in *Proceedings of NATO ARW on Unsaturated Flow in Hydrological Modelling*, edited by H. J. Morel-Seytoux, pp. 191–219, Kluwer, Dordrecht, Netherlands.

Beven, K. J. (2001), *Rainfall-Runoff Modelling—The Primer*, Wiley, New York.

Beven, K. J. (2006), The holy grail of scientific hydrology: Q = H(SR) A as a closure, *Hydrol. Earth Syst. Sci.*, *10*, 609–618.

Botter, G., E. Bertuzzo, A. Bellin, and A. Rinaldo (2005), On the Lagrangian formulations of reactive solute transport in the hydrologic response, *Water Resour. Res.*, *41*, W04008, doi:10.1029/2004WR003544.

Botter, G., T. Settin, M. Marani, and A. Rinaldo (2006), A stochastic model of nitrate transport and cycling at basin scale, *Water Resour. Res.*, *42*, W04415, doi:10.1029/2005WR004599.

Botter, G., A. Porporato, I. Rodriguez-Iturbe, and A. Rinaldo (2007), Basin-scale soil moisture dynamics and the probabilistic characterization of carrier hydrologic flows: Slow, leaching-prone components of the hydrologic response, *Water Resour. Res.*, *43*, W02417, doi:10.1029/2006WR005043.

Botter, G., F. Peratoner, M. Putti, A. Zuliani, R. Zonta, A. Rinaldo, and M. Marani (2008a), Observation and modeling of catchment-scale solute transport in the hydrologic response: A tracer study, *Water Resour. Res.*, *44*, W05409, doi:10.1029/2007WR006611.

Botter, G., E. Daly, A. Porporato, I. Rodriguez-Iturbe, and A. Rinaldo (2008b), Probabilistic dynamics of soil nitrate: Coupling of ecohydrological and biogeochemical processes, *Water Resour. Res.*, *44*, W03416, doi:10.1029/2007WR006108.

Botter, G., S. Milan, G. Botter, M. Marani, and A. Rinaldo (2009), Inferences from catchment-scale tracer circulation experiments, *J. Hydrol.*, *369*(3–4), 368–380, doi:10.1016/j.jhydrol.2009.02.012.

Brutsaert, W., and J. L. Nieber (1977), Regionalized drought flow hydrographs from a mature glaciated plateau, *Water Resour. Res.*, *13*(3), 637–648.

Burns, D. A., R. B. Hooper, J. J. McDonnell, J. E. Freer, C. Kendall, and K. Beven (1998), Base cation concentrations in subsurface flow from a forested hillslope: The role of flushing frequency, *Water Resour. Res.*, *34*(12), 3535–3544.

Cirmo, C. P., and J. J. McDonnell (1998), Linking the hydrologic and biogeochemical controls of nitrogen transport in near-stream zones of temperate-forested catchments: A review, *J. Hydrol.*, *199*, 88–120.

Cvetkovic, V., and G. Dagan (1994), Transport of kinetically sorbing solute by steady velocity in heterogeneous porous formations, *J. Fluid Mech.*, *265*, 189–215.

Dagan, G. (1989), *Flow and Transport in Porous Formations*, Springer, New York.

Evans, C., and T. D. Davies (1998), Causes of concentration/discharge hysteresis and its potential as a tool for analysis of episode hydrochemistry, *Water Resour. Res.*, *34*(1), 129–137.

Fiori, A., and D. Russo (2008), Travel time distribution in a hillslope: Insight from numerical simulations, *Water Resour. Res.*, *44*, W12426, doi:10.1029/2008WR007135.

Godsey, S. E., J. W. Kirchner, and D. W. Clow (2009), Concentration-discharge relationships reflect chemostatic characteristics of US catchments, *Hydrol. Processes*, *23*, 1844–1864, doi:10.1002/hyp.7315.

Gupta, A., and V. Cvetkovic (2000), Temporal moment analysis of tracer discharge in streams: Combined effect of physiochemical mass transfer and morphology, *Water Resour. Res.*, *36*(10), 2985–2997.

Gupta, A., and V. Cvetkovic (2002), Material transport from different sources in a network of streams through a catchment, *Water Resour. Res.*, *38*(7), 1098, doi:10.1029/2000WR000064.

Gupta, V. K., and E. C. Waymire (1993), A statistical analysis of mesoscale rainfall as a random cascade, *J. Appl. Meteorol.*, *32*, 251–267.

Gupta, V. K., E. Waymire, and C. T. Wang (1980), A representation of an IUH from geomorphology, *Water Resour. Res.*, *16*(5), 862–885.

Kirchner, J. W. (2009), Catchments as simple dynamical systems: Catchment characterization, rainfall-runoff modeling, and doing hydrology backward, *Water Resour. Res.*, *45*, W02429, doi:10.1029/2008WR006912.

Laio, F., A. Porporato, L. Ridolfi, and I. Rodriguez-Iturbe (2001), Plants in water-controlled ecosystems: Active role in hydrologic processes and response to water stress. Part II. Probabilistic soil moisture dynamics, *Adv. Water Resour.*, *24*(7), 707–723.

Leaney, F. W., K. R. J. Smettem, and D. J. Chittleborough (1993), Estimating the contribution of preferential flow to subsurface runoff from a hillslope using deuterium and chloride, *J. Hydrol.*, *147*(1–4), 83–103.

Lindgren, G. A., G. Destouni, and A. V. Miller (2004), Solute transport through the integrated groundwater-stream system of a catchment, *Water Resour. Res.*, *40*, W03511, doi:10.1029/2003WR002765.

Maloszewski, P., and A. Zuber (1982), Determining the turnover time of groundwater systems with the aid of environmental tracers. Part 1. Models and their applicability, *J. Hydrol.*, *57*, 207–231.

Maloszewski, P., W. Rauert, P. Trimborn, A. Herrmann, and R. Rau (1992), Isotope hydrological study of mean transit times in an alpine basin (Wimbachtal, Germany), *J. Hydrol.*, *140*, 343–360.

McDonnell, J. J. (1990), A rationale for old water discharge through macropores in a steep, humid catchment, *Water Resour. Res.*, *26*, 2821–2832.

McDonnell, J. J., I. F. Owens, and M. K. Stewart (1991), A case study of shallow flow paths in a step zeroth-order basin: A phisical-chemical-isotopic analysis, *Water Resour. Bull.*, *27*, 679–685.

McGlynn, K. J., J. J. McDonnell, M. K. Stewart, and J. Seibert (2003), On the relationships between catchment scale and streamwater mean residence time, *Hydrol. Processes*, *17*, 175–181.

McGuire, K. J., and J. J. McDonnell (2006), A review and evaluation of catchment transit time modeling, *J. Hydrol.*, *330*, 543–563, doi:10.1026/j.hydrol.2006.04.020.

McGuire, K. J., D. R. DeWalle, and W. J. Gburek (2002), Evaluation of mean residence time in subsurface waters using oxygen-18 fluctuations during drought conditions in the mid-Appalachians, *J. Hydrol.*, *261*, 132–149.

McGuire, K. J., M. Weiler, and J. J. McDonnell (2007), Integrating tracer experiments with modeling to assess runoff processes and water transit times, *Adv. Water Resour.*, *30*(4), 824–837.

Molnar, P., and P. Burlando (2005), Preservation of rainfall properties in stochastic disaggregation by a simple random cascade model, *Atmos. Res.*, *77*(1–4), 137–151.

Mulholland, P. J., et al. (2008), Stream denitrification across biomes and its response to anthropogenic nitrate loading, *Nature*, *452*(13), 202–205.

Niemi, A. J. (1977), Residence time distribution of variable flow processes, *Int. J. Appl. Radiat. Isot.*, *28*, 855–860.

Nyberg, L., A. Rodhe, and K. Bishop (1999), Water transit times and flow path from two line injections of ^{3}H and ^{36}Cl in a microcatchment at Gardsjön, Sweden, *Hydrol. Processes*, *13*, 1557–1575.

Peters, N. E., and E. B. Ratcliffe (1998), Tracing hydrologic pathways using chloride at Panola Mountain Research Watershed, Georgia, USA, *Water Air Soil Pollut.*, *105*(1–2), 263–275.

Porporato, A., E. Daly, and I. Rodrguez-Iturbe (2004), Soil water balance and ecosystem response to climate change, *Am. Nat.*, *164*(5), 625–633.
Rinaldo, A., and M. Marani (1987), Basin scale model of solute transport, *Water Resour. Res.*, *23*(11), 2107–2118.
Rinaldo, A., A. Bellin, and M. Marani (1989), On mass response functions, *Water Resour. Res.*, *25*(8), 1603–1617.
Rinaldo, A., A. Marani, and R. Rigon (1991), Geomorphological dispersion, *Water Resour. Res.*, *28*, 513–525.
Rinaldo, A., G. Botter, E. Bertuzzo, A. Uccelli, T. Settin, and M. Marani (2006a), Transport at basin scales: Part 1. Theoretical framework, *Hydrol. Earth Syst. Sci.*, *10*, 19–30.
Rinaldo, A., G. Botter, E. Bertuzzo, A. Uccelli, T. Settin, and M. Marani (2006b), Transport at basin scales: Part 2. Applications, *Hydrol. Earth Syst. Sci.*, *10*, 31–48.
Rodhe, A., L. Nyberg, and K. Bishop (1996), Transit times for water in a small till catchment from a 16 step shift in the oxygen 18 content of the water input, *Water Resour. Res.*, *32*(12), 3497–3511.
Rodriguez-Iturbe, I., and A. Porporato (2004), *Ecohydrology of Water Controlled Ecosystems: Soil Moisture and Plant Dynamics*, Cambridge Univ. Press, New York.
Rodriguez-Iturbe, I., and A. Rinaldo (1997), *Fractal River Basins: Chance and Self-Organization*, Cambridge Univ. Press, New York.
Rodriguez-Iturbe, I., and J. B. Valdes (1979), The geomorphologic structure of hydrologic response, *Water Resour. Res.*, *15*(6), 1409–1420.
Rodriguez-Iturbe, I., A. Porporato, L. Ridolfi, V. Isham, and D. Cox (1999), Probabilistic modelling of water balance at a point: The role of climate soil and vegetation, *Proc. R. Soc. London, Ser. A*, *455*, 3789–3805.
Russo, D., and A. Fiori (2009), Stochastic analysis of transport in a combined heterogeneous vadose zone-groundwater flow system, *Water Resour. Res.*, *45*, W03426, doi:10.1029/2008WR007157.
Settin, T., G. Botter, I. Rodriguez-Iturbe, and A. Rinaldo (2007), Numerical studies of soil moisture distributions in heterogeneous catchments, *Water Resour. Res.*, *43*, W05425, doi:10.1029/2006WR005737.
Sherman, L. K. (1932), Streamflow from rainfall by unit-graph method, *Eng. News Rec.*, *108*, 501–505.
Stewart, M. K., and J. J. McDonnell (1991), Modeling base-flow soil-water residence times from deuterium concentrations, *Water Resour. Res.*, *27*(10), 2681–2693.
Stumpp, C., W. Stichler, and P. Maloszewski (2009), Application of the environmental isotope δ^{18}O to study water flow in unsaturated soils planted with different crops: Case study of a weighable lysimeter from the research field in Neuherberg, Germany, *J. Hydrol.*, *368*, 68–78, doi:10.1016/j.hydrol.2009.01.027.
Taylor, G. I. (1921), Diffusion by continuous movements, *Proc. London Math. Soc., Ser. A*, *20*, 196–211.
Weiler, M., and J. J. McDonnell (2006), Testing nutrient flushing hypotheses at the hillslope scale: A virtual experiment approach, *J. Hydrol.*, *319*, 339–356.
Weiler, M., B. L. McGlynn, K. J. McGuire, and J. J. McDonnell (2003), How does rainfall become runoff? A combined tracer and runoff transfer function approach, *Water Resour. Res.*, *39*(11), 1315, doi:10.1029/2003WR002331.
Wilson, G. V., et al. (1991a), Hydrogeochemical processes controlling subsurface transport from an upper subcatchment of walker branch watershed during storm events. Part 1. Hydrologic transport processes, *J. Hydrol.*, *123*, 297–316.
Wilson, G. V., et al. (1991b), Hydrogeochemical processes controlling subsurface transport from an upper subcatchment of walker branch watershed during storm events. Part 2. Solute transport processes, *J. Hydrol.*, *123*, 317–336.

E. Bertuzzo, Laboratory of Ecohydrology, Faculté ENAC, Ecole Polytechinque Federale, Bâtiment GR, Station 2, CH-1015 Lausanne, Switzerland. (andrea.rinaldo@epfl.ch)

G. Botter and A. Rinaldo, Dipartimento di Ingegneria Idraulica Marittima Ambientale e Geotecnica, Università degli Studi di Padova, Via Loredan 20, I-35131 Padua, Italy. (botter@idra.unipd.it; rinaldo@idra.unipd.it)